blood–brain barrier, although formal testing is needed to ascertain these issues. The emergence of highly resistant HIV-1 variants may not readily arise since the active anti-HIV 4′-SdNs with a smaller substituent at the 4′-position have structures more similar to dN.

If this speculation is true, we can design and discover novel NRTIs which are able to prevent, or delay, emergence of drug-resistant virus.

Design and synthesis of 4′-CNdNs from natural 2′-deoxynucleosides

From previous studies on SAR of 4′-*C*-substituted nucleosides, it was expected that a smaller substituent at the *C*-4′ position would give more acceptable biological activity. This is based on the parameter $-\Delta G^0$ values between equatorial and axial substituents on the cyclohexane rings. Thus, purine 2′-deoxynucleoside derivatives bearing a cyano group, which might be smaller than an ethynyl one (at the *C*-4′-position), will have more potent antiviral activity. During our synthesis of 4′-*C*-substituted nucleosides, we have been utilizing a glycosidation reaction of 4-*C*-substituted sugar derivatives with nucleobases. However, this synthetic route incurs some problems (Figure 11).

Synthetic problems in the condensation method are summarized as follows:

1) Preparation of 4′-*C*-substituted sugars and their derivation to the desired nucleosides require multi-step reactions and their total yields are low.

2) 4′-*C*-Substituted sugars have low reactivity in glycosidation reaction, especially when their substituent is an electron-withdrawing group like a cyano group.

These problems prompted us to develop a preparation method of 4′-*C*-substituted purine nucleosides from the corresponding nucleosides. This approach enabled us to synthesize 4′-*C*-cyano purine nucleoside derivatives, which were difficult to synthesize by condensation of sugars with nucleobases.

Synthesis of 4′-C-cyano-2′-purine-nucleosides. The synthesis of 4′-*C*-cyano-2′-purine-nucleosides starting from 2′-deoxyadenosine and dDAP is shown (Figure 12). The key intermediates **[81a,b]** for the synthesis of 4′-*C*-ethynyl- and 4′-*C*-cyano-purine-2′-deoxynucleosides were prepared according to Matsuda's procedure, with some modifications (Nomura *et al.*, 1999). The hydroxymethyl group of the key intermediate **[81a]** was converted to a cyano group. A 4′-*C*-formyl derivative, which was obtained by Moffatt oxidation of the hydroxymethyl group in **[81a]**, was converted to a 4′-*C*-aldoxime derivative and then further dehydrated to give 4′-*C*-cyano derivative **[82a]**. The protecting groups of compound **[82a]** were removed to give 2′-deoxyadenosine derivative (4′-CNdA) **[83a]**. Additionally, 4′-*C*-cyano-2,6-diaminopurine 2′-deoxyriboside (4′-CNdDAP) **[83b]** was also synthesized by a similar procedure to that described for compound **[83a]**. The cyano derivatives **[83a,b]** were readily converted to 2′-deoxyinosine (4′-CNdI) **[84a]** and 2′-deoxyguanosine derivatives (4′-CNdG) **[84b]** by enzymatic deamination.

Synthesis of 4′-EdNs from 2′-deoxynucleosides. These synthetic methods using nucleosides as the starting material were also an effective route to the various 4′-*C*-ethynyl derivatives 4′-EdA **[86a]**, 4′-EdI **[87a]**, 4′-EdDAP **[86b]** and 4′-EdG **[87b]** (Figure 12). It will be easy for us to scale up the process for the preparation of 4′-*C*-ethynyl derivatives.

In summary, we developed a method for preparing purine 2′-deoxynucleoside derivatives bearing an ethynyl or a cyano group at the 4′ position from the corresponding 2′-deoxynucleosides as the starting materials. The total yields of 4′-*C*-substituted purine nucleosides were improved (compared to that of the condensation method of sugars with bases) by using this synthetic route. Furthermore, it became easy to make derivatives bearing an electron-withdrawing substituent like a cyano group.

Anti-HIV activity of 4′-CNdNs. The activity of 4′-CNdNs, together with that of 4′-EdNs, is shown in Table 2. Unfortunately, the anti-HIV activity of 4′-CNdNs did not meet our expectations. In the case of 4′-EdA **[86a]**, it was easily hydrolysed to give 4′-EdI **[87a]**, which was less active than the parent 4′-EdA **[86a]**. In contrast, 4′-CNdI **[84a]** was as potent as 4′-CNdA **[83a]** against HIV-1 despite the low activity of 4′-EdI **[87a]**.

Attempts to synthesize less toxic and/or stable analogues

Design and synthesis of L-4′-EdNs (L-4′-EdDAP [92], dG [93], and dC [98]). During our exploration of novel NRTIs, we selected 4′-ethynyl-2′-deoxy-purine-nucleoside (2,6-diaminopurine derivative **[86b]** and guanine derivative **[87b]**) for *in-vivo* assay because of their high biological activity *in vitro*. However, they showed high toxicity in mice (Ashida, Yamasa Corporation, personal communication). Additionally, 4′-*C*-cyano-2′-deoxy-purine-nucleoside (2,6-diaminopurine derivative **[83b]** and guanine derivative **[84b]**) were very toxic in the *in-vitro* assay (Ashida, Yamasa Corporation, personal communication). On the other hand, Chu *et al.* reported that the enantiomer of 3TC (D-enantiomer) was very toxic, but 3TC itself (L-enantiomer) was less toxic (Beach *et al.*, 1992). Therefore, we designed and synthesized L-4′-ethynyl derivatives such as **[92]** and **[93]** in an effort to reduce toxicity (Figure 13) (Kitano, Yamasa Corporation, private communication). Synthesis of the L-ribose unit bearing an ethynyl group at the 4-*C*-position and the glycosidation are outlined (Figure 13).

Table 2. Anti-HIV activity of 4′-*C*-cyano and 4′-*C*-ethynyl purine nucleosides

Compound	Anti-HIV activity*		
	EC_{50} (μM)	CC_{50} (μM)	Selectivity index
4′-ethynyl dA **[86a]**	0.0098	16	1633
4′-ethynyl dDAP **[86b]**	0.00034	0.9	2647
4′-ethynyl dI **[87a]**	0.13	137	1054
4′-ethynyl dG **[87b]**	0.0015	1.4	933
4′-cyano dA **[83a]**	0.051	12	235
4′-cyano dDAP **[83b]**	0.00079	>0.034	>43
4′-cyano dI **[84a]**	0.051	23	451
4′-cyano dG **[84b]**	0.000188	>0.034	>181
zidovudine (AZT)	0.0032	29.4	9188

*Anti-HIV activity was determined by MTT assay. MT-4 cells and HIV-1_{LAI} were employed.

Figure 12. Synthesis of 4′-*C*-cyano and 4′-*C*-ethynyl purine 2′-deoxynucleosides by modification of natural nucleosides

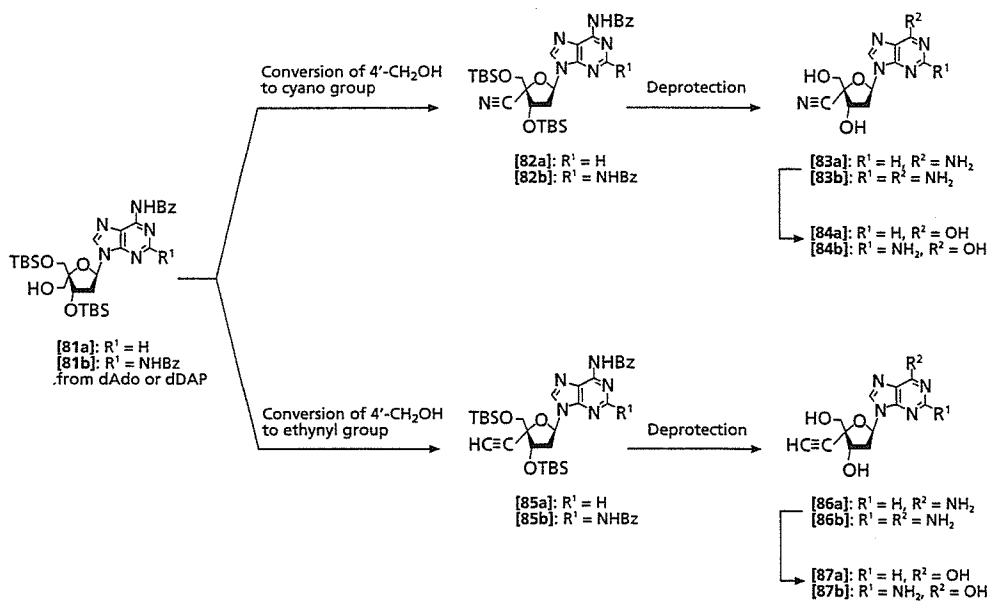

4-C-Hydroxymethyl-3,5-di-O-benzyl-1,2-O-isopropylidene-α-L-ribo-pentofuranose [89]. The key intermediate, was obtained from D-arabinose in nine steps. Silylation and isopropylidenation of D-arabinose gave 5-*O*-TBDPS-1,2-*O*-isopropylidene-α-D-*arabino*-pentofuranose **[88]** in two steps. The inversion of the 3-hydroxyl group in compound **[88]** gave D-lyxo-pentofuranose derivative, which was derived to the key intermediate **[89]** by introduction of a hydroxymethyl group into the *C*-4 position by Moffatt's procedure and the following selective benzylation of the 5-hydroxyl group. L-Enantiomers of 4′-*C*-ethynyl dDAP **[92]** and dG **[93]** were obtained from the key intermediate **[89]** by a known procedure (Kohgo *et al.*, 1999; Ohrui *et al.*, 2000).

On the other hand, 4′-*C*-ethynyl-2′-deoxycytidine (4′-EdC) **[22]** had very potent anti-HIV activity, but this compound also showed cytotoxicity. Therefore, L-4′-*C*-ethynyl-2′-deoxycytidine (L-4′-EdC) **[98]** was also prepared from D-glucose by us (Figure 14) (Kohgo *et al.*, 2001). The synthetic scheme is summarized (Figure 14).

The L-enantiomers of 4′-*C*-ethynyl-2′-deoxynucleosides **[92, 93, 98]** were evaluated for anti-HIV activity toward MT-2 or MT-4 cells by an MTT assay. However, all these nucleosides were inactive against HIV-1 at concentrations up to 100 μM. It is worth noting none of the L-isomers of 4′-EdNs showed significant antiviral activity against HIV-1 *in vitro*.

Design and synthesis of 4′-C-substituted-6-chloropurine nucleosides (4′-S-6-CldNs) [101a,b] and 4′-C-substituted-6-mercapto-purine nucleosides (4′-S-6-SHdNs) [103a,b]. Additionally, we also chose 4′-EdA **[86a]** as another candidate because of its activity in the *in vitro* assay, but it was metabolized immediately *in vivo* to give the less active 4′-EdI **[87a]**. Thus, we attempted to resolve the above metabolic problem by a different approach. As mentioned above, while the anti-HIV activity of 4′-CNdNs did not meet our expectations, 4′-CNdI **[84a]** did prove active against HIV-1. Therefore, we focused on the modification at the 6-position of purine nucleosides in the case of 4′-ethynyl- and cyano-derivatives.

We previously confirmed that 6-chloro-purine-nucleosides were easily hydrolysed by adenosine deaminase (ADA) to give inosine derivatives. However, it was reported that 6-mercaptopurine-nucleosides were tolerant to this reaction (Murakami *et al.*, 1991). Furthermore, they also reported the modification method at the 6-position of purine dideoxynucleosides by chloro and mercapto groups to increase lipophilicity for these compounds (Murakami *et al.*, 1991). Therefore, we designed the modification at the 6-position of purine nucleosides utilizing their method. The preparation method for 4′-*C*-substituted 6-chloro-purine and 6-mercapto-purine derivatives is summarized in Figure 15.

We selected 4′-EdA derivative **[99a]** and 4′-CNdA derivative **[99b]** as key intermediates. The 6-amino group in 4′-EdA **[99a]** or 4′-CNdA derivatives **[99b]** were converted to a chloro group with Et_4NCl-tBuONO to give protected 6-chloro derivative **[100a,b]**. These derivatives **[100a,b]** were deprotected with ammoniumfluoride hydrogen fluoride (NH_4F-HF) in methanol or tetrabuthylammonium fluoride (TBAF) in THF to give the desired nucleosides **[101a,b]**.

Protected 6-chloro-purine derivatives **[100a,b]** were also used to prepare 6-mercapto-purine derivatives **[103a,b]**. Protected 4′-E- and 4′-CN-6-mercaptopurine analogues **[102a,b]** were obtained by the reaction of **[100a,b]** with sodium hydrosulphide in distilled water/ethanol or thiourea in refluxing ethanol, and the following deprotection of **[102a,b]** gave 4′-E- and 4′-CN-6-mercaptopurine derivatives **[103a,b]**.

Unfortunately, while 6-Cl purine derivative **[101a,b]** still showed weak activity, 6-mercapto derivatives **[103a,b]** exerted no anti-HIV-1 activity *in vitro*. The lack of antiretroviral activity of these nucleosides **[101a,b; 103a,b]** may be due to them not being converted to the desired analogues of 4′-*C*-substituted-dG or dI. According to Murakami *et al.*, (1991) 2-amino-6-mercapto-ddNs are not substrates for ADA nor is it converted to ddG at all in the presence of an excess of isolated ADA.

Design and synthesis of α-L-4′-CNdNs (Kohgo, Yamasa Corporation, private communication). Inversion of the configuration at the 4′-*C* of the sugar leads to the α-L-series of nucleosides; therefore, we made alpha-L-4′-*C*-cyano-2′-deoxyadenosine. Unfortunately, α-L-4′-CNdNs did not show anti-HIV activity. Synthesis in our laboratory of α-L-4′-EdNs is in progress.

As can be seen from the results mentioned above, 4′-*C*-ethynyl- and 4′-cyano-nucleosides are promising candidates among various 4′-*C*-substituted nucleosides. Therefore, finally we describe the crucial factors (drug resistance, stability, mode of actions, toxicity and bulkiness) which will influence the development of the 4′-*C*-ethynyl-nucleosides and other 4′-SdNs.

Drug resistance

Activity of 4′-SdNs against drug-resistant infectious HIV-1 clones

The activity of selected 4′-SdNs against HIV-1 variants resistant to various NRTIs using MAGI assay is listed (Table 3). It is noteworthy that the three cytosine analogues, 4′-EdC **[22]**, 4′-EaraC **[79]** and 4′-MdC **[27]** suppressed the replication of HIV-1_{K65R}, HIV-1_{L74V}, HIV-$1_{M41L/T215Y}$ and multi-dideoxynucleoside-resistant HIV-$1_{A62V/V75I/F77L/F116Y/Q151M}$ (MDR) at EC_{50} values ranging

Figure 13. Synthesis of L-4′-*C*-ethynyl purine 2′-deoxynucleosides from D-arabinose

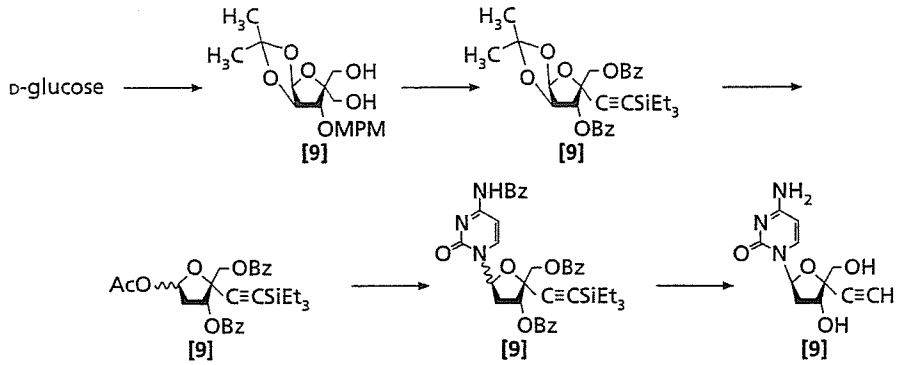

Figure 14. Synthesis of L-enantiomer of 4′-*C*-ethynyl-2′-deoxycytidine from D-glucose

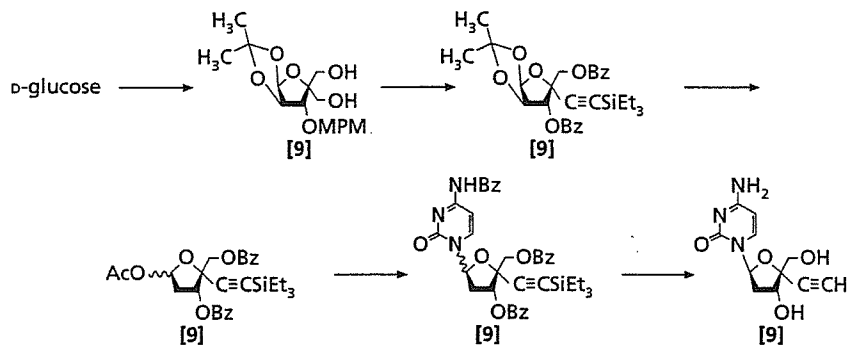

Table 3. Antiviral activity of 4′-C-substituted nucleosides against drug-resistant infectious clones

Compound	EC_{50} (μM)*									CC_{50} (μM)
	HXB2	K65R	L74V	M41L/T215Y	M184V	M184I	M41L/T69S-S-G/T215Y	MDR	Y181C	
Pyrimidine analogues										
4′-ET										
[28]	0.36	0.53	0.68	0.43	0.18	0.14	0.44	0.12	0.13	>200
4′-EdC										
[22]	0.0012	0.0008	0.0013	0.006	0.0024	0.0026	0.015	0.0012	0.0021	>200
4′-EaraC										
[79]	0.0071	0.015	0.026	0.026	0.71	0.48	0.17	0.0079	0.016	>200
4′-MdC										
[27]	0.0058	0.0071	0.0062	ND	0.2	0.74	ND	0.0033	ND	>200
4′-FMdC										
[73]	0.0046	0.065	0.0019	0.0035	2.0	ND	0.066	0.0039	ND	>200
Purine analogues										
4′-EdA										
[86a]	0.008	0.033	0.004	0.012	0.047	0.022	0.065	0.0062	0.011	>200
4′-EdDAP										
[86b]	0.0014	0.00035	0.0007	0.0017	0.0059	0.0027	0.0041	0.001	0.0008	>200
4′-EdI										
[87a]	0.81	0.25	0.61	1.3	16.6	1.5	2.2	0.51	ND	>200
4′-EdG										
[87b]	0.007	0.001	0.0012	0.019	0.008	0.0041	0.0068	0.0048	0.01	52
4′-CNdA										
[83a]	0.043	ND	ND	ND	2.28	ND	ND	0.083	ND	ND
4′-CNdI										
[84a]	0.242	ND	ND	ND	6.06	ND	ND	0.296	ND	ND
AZT	0.022	0.02	0.02	0.3	0.01	0.017	1.6	15.3	0.014	>100
ddC	0.2	3.0	1.5	ND	2.2	ND	1.3	5.5	ND	>100
3TC	0.71	ND	ND	ND	>100	>100	9.9	1.1	ND	>100
ddI	3.9	12.7	19.5	3.6	10.1	ND	12.2	25	ND	>100

*Anti-HIV activity was determined with the MAGI assay. ND, not determined.

Table 4. Antiviral activity of 4′-*C*-ethynyl nucleosides against clinical isolates

Strain	Amino acid substitution(s)		EC_{50} (μM)*			
	RT region	Protease region	4′-EdC **[22]**	4′-EdA **[86a]**	4′-EdDAP **[86b]**	AZT
ERS_{104pre}	None	None	0.0012	0.013	0.00083	0.0056
IVR_{205}	None	K20M, M36I, D60E	0.0023	0.0034	0.0001	0.0015
IVR_{207}	G190Q	V77I	0.0046	0.0022	<0.0001	0.0036
Pt1	T69G, K70R, L74V, A98G, K103N, V179D, M184V, T215F, K219F	L10I, L33I, M36I, M46I, L36P, A71V, G73S, V82A, L90M	0.00064 (0.5-fold)	0.00054 (0.4-fold)	0.0011 (1.3-fold)	0.029 (52-fold)
Pt6	M41L, D67N, M184V, L210W, T215Y	L10I, K20R, L24I, M36I, M46L, I54V, L63P, V82A, L89M	0.013 (11-fold)	0.040 (3-fold)	0.0001 (0.1-fold)	0.28 (50-fold)
Pt7	M41L, D67N, T69D, M184V, T215F	L10I, K45R, I54V, L63P, A71V, V82T, L90M	0.0016 (1.3-fold)	0.009 (0.7-fold)	0.0005 (0.6-fold)	1.9 (340-fold)
Pt9	M41L, M184V, T215Y	M46I, L63P, A71V, V77I, I84V, N88D, L90M	0.023 (19-fold)	0.029 (2.2-fold)	0.0031 (3.7-fold)	0.97 (170-fold)

*EC_{50}s were determined with PHA-PBMC. Numbers in parentheses represent fold changes of EC_{50}s against each HIV-1 isolate compared to those against the wild-type clinical HIV-1 strain, $ERS_{104pre+}$.

from 0.001–0.015 μM. Among these nucleosides, only 4′-EdC **[22]** remained active against 3TC-resistant HIV-1_{M184I} and HIV-1_{M184V} but was less active against MDR-HIV-$1_{M41L/T69S\text{-}S\text{-}G/T215Y}$ than other variants, while 4′-EdC **[22]** remained potent against MDR-HIV-$1_{M41L/T69S\text{-}S\text{-}G/T215Y}$. The three purine analogues (4′-EdA) **[86a]**, 4′-EdDAP **[86b]** and 4′-EdG **[87b]** that were potent against wild-type HIV-1 were also highly active against all the infectious clones. Additionally, they were also active against a non-nucleoside RTI-resistant (NNRTI) infectious HIV-1_{Y181C}.

Activity of 4′-SdNs against HIV-1 isolated from heavily drug-experienced patients with AIDS

The *in vitro* activity of the three most potent 4′-E-nucleosides (Table 4), 4′-EdC **[22]**, 4′-EdA **[86a]** and 4′-EdDAP **[86b]** was tested against multi-drug resistant clinical HIV-1 variants isolated from heavily drug-experienced patients with AIDS. All three 4′-E-nucleosides suppressed replication of these highly drug-resistant clinical strains isolated from patients 1 and 7 as effectively as those of the wild-type clinical strain HIV-$1_{ERS104pre}$.

Properties and pharmacokinetics of 4′-EdNs and 4′-CNdNs

Stability of 4′-SdNs against enzymatic catabolism. It took 4 h to completely deaminate 4′-EdA **[86a]**. Under the same conditions, the enzyme, adenosine deaminase, deaminated ddA in 2 h. Pyrimidine phosphorylase hydrolysed 4′-*C*-methyl-2′-deoxy-5-ethyluridine by only 6% under conditions where the enzyme hydrolysed arabinofuranosyl-5-ethyluridine by 53% and 2′-deoxy-5-ethyl-uridine completely. All attempts for enzymatic exchange of the base of 4′-ET **[28]** with adenine were unsuccessful because the glycosyl linkage of 4′-ET **[28]** was too stable to be cleaved by the enzymes used. 4′-SdNs are fairly stable under physiological conditions, although the catabolism of 4′-SdNs following triphosphorylation as yet remains to be determined.

Stability of 4′-SdNs (mainly 4′-EdNs) under acidic conditions. When three 4′-EdNs (4′-EdC 22, 4′-EdA) **[86a]**, and 4′-EdDAP **[86b]** and two ddNs (ddI and AZT) were exposed to 1M HCl for up to 20 min and then to 1M NaOH, their anti-HIV-1 activity was then tested. All 4′-EdNs were active although the acid-labile ddI completely lost its antiviral activity. The acid-stable property of these 4′-SdNs may contribute favourably to their oral bioavailability, if they are ultimately administered orally.

Mode of actions of 4′-SdNs. 4′-SdNs act as NRTIs and terminators of viral DNA biosynthesis in spite of the presence of the 3′α-OH group. Although a variety of side effects of NRTIs, some of which are often lethal, are well known and attributed to the inhibitory effect of ddN-TPs on mitchondrial polymerase γ activity, such effect has yet to be determined for 4′-SdNs. Such data regarding polymerase γ inhibition of 4′-SdNs-TPs are essential before 4′-SdNs may be considered as potential therapeutics for HIV-1 infection.

4′-E-nucleosides examined in our study retain the 3′-OH moiety like natural substrates, which may enable 4′-E-nucleosides to interact with the mutated 3′-OH binding site of various types of drug-resistant HIV.

Toxicity. It should be noted, however, since 4′-SdNs have the 3′-OH moiety, that the incorporation of 4′-SdNs to cellular and mitochondrial DNA may be more likely to happen, thus causing higher levels of unacceptable toxicity compared with ddNs. 4′-EdDAP **[86b]**, 4′-EdG **[87b]**, 4′-CNdDAP **[83b]** and 4′-CNdG **[84b]** were very toxic. Fortunately, 4′-EdA **[86a]**, 4′-EdI **[87a]**, 4′-CNdA **[83a]** and 4′-CNdI **[84a]** were less toxic.

Bulkiness. The results indicate that the structures of 4′-SdNs with a less sterically demanding substituent at the 4′-position are closer to the structures of dNs and have greater anti-HIV activity. However, the 4′-CN derivative did not meet our expectations. The expected properties come from the presence of 4′-substituents.

Conclusions

As can be seen from the research histories of various 4′-SdNs, novel NRTIs such as either 4′-EdNs (by us) and 4′-Ed4T **[47]** (by M Tanaka's group) appear to have sufficient anti-HIV-1 potency and favourable pharmacological properties. Therefore, they may be promising candidate therapeutics for HIV-1 infection and may be active against presently existing drug-resistant HIV-1 strains.

It should be noted that several issues, such as inhibition of mitochondrial DNA synthesis by 4′-SdNs-TPs (due to polymerase γ inhibition by 4′-SdNs-TPs) and pharmacokinetics, remain to be addressed before these analogues are considered for further development. However, we believe that NRTIs, especially 4′-EdNs, 4′-CNdNs and 4′-Ed4T **[47]**, may be considered as potential therapeutics for HIV-1 infection. It is also noteworthy that 4′-Ed4T **[47]** is less toxic to CEM cell growth and less inhibitory to mitochondrial DNA synthesis than d4T. Further searches for NRTIs are in progress in our laboratory.

Acknowledgements

The authors are grateful to Dr K Kodama of Yamasa Corporation for his encouragement throughout this work. Thanks are also due to Dr T Waga, Dr S Sakata, Dr K

Figure 15. 4′-C-substituted 6-chloro and 6-mercapto purine nucleosides

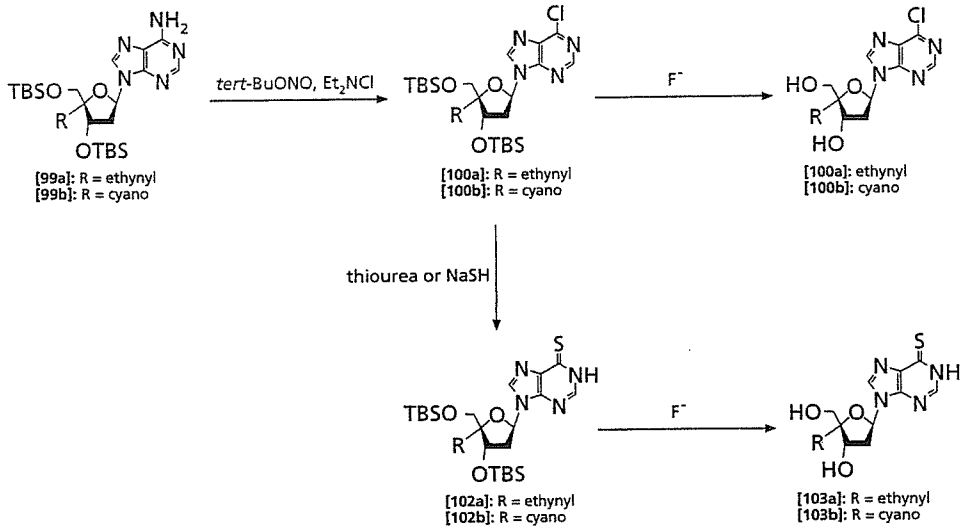

Yamada, Mr N Matsumoto for synthetic experiments, Dr S Shigeta, Dr M Saneyoshi, Dr T Yamaguchi, Dr M Matsuoka, Mr D Nameki, Dr T Abiru and Dr H Machida for biological studies.

References

Beach JW, Jeong LS, Alves AJ, Pohl D, Kim HO, Chang C-N, Doong S-L, Schinazi RF, Cheng Y-C & Chu CK (1992) Synthesis of enantiomerically pure (2′R, 5′S)-(-)-1-[2-(hydroxymethyl)oxathiolan-5-yl]cytosine as a potent antiviral agent against hepatitis B virus (HBV) and human immunodeficiency virus (HIV). *Journal of Organic Chemistry* **57**:2217–2219.

Chen MS, Suttmann RT, Papp E, Cannon PD, McRoberts MJ, Bach C, Copeland WC & Wang TS (1993) Selective action of 4′-azidothymidine triphosphate on reverse transcriptase of human immunodeficiency virus type 1 and human DNA polymerases alpha and beta. *Biochemistry* **32**:6002–6010.

Crich D & Hao X (1999) Asymmetric synthesis of C4′α-carboxylated 2′-deoxynucleosides. Preparation of oxetanone derivatives and influence of solvent on the stereochemistry of base introduction. *Journal of Organic Chemistry* **64**:4016–4024.

Haraguchi K, Itoh Y, Takeda S, Honma Y, Tanaka H, Nitanda T, Baba M, Dutschman GE & Cheng Y-C (2004) Synthesis of anti-HIV activity of agent 4′-cyano-2′, 3′-didehydro-3′-deoxythymidine. *Nucleosides Nucleotides & Nucleic Acids* **23**:647–654.

Haraguchi K, Takeda S, Tanaka H, Nitanda T, Baba M, Dutschman GE & Cheng Y-C (2003) Synthesis of a highly active new anti-HIV agent 2′,3′-didehydro-3′-deoxy-4′-ethynylthymidine. *Bioorganic & Medicinal Chemistry Letters* **13**:3775–3777.

Haraguchi K, Tanaka H, Ito Y, Saito S & Miyasaka T (1992) Stereoselective synthesis of 4′-*C*-branched 2′,3′-didehydro-2′,3′-dideoxy nucleosides based on SnCl4-promoted allylic rearrangement. *Tetrahedron Letters* **33**:2841–2844.

Hrebabecky H & Holy A (1993) Synthesis of 1-(3-azido-2, 3-dideoxy-4-*C*-hydroxymethyl-α-L-threo-pentofuranosyl)thymine, 1-(2,3-dideoxy-4-*C*-hydroxymethyl-α-L-glycero-pentofuranosyl)thymine and 1-(2,3-dideoxy-4-*C*-hydroxymethyl-α-L-glycero-pent-2-enofuranosyl)thymine. *Collection of Czechoslovak Chemical Communications* **58**:409–420.

Imanishi T & Obika S (1999) Syntheses and properties of novel conformationally restrained nucleoside analogues. *Journal of Synthetic Organic Chemistry Japan* **57**:969–980.

Jenkins ID, Verheyden, JPH & Moffatt JG (1976) 4′-Substituted nucleosides. 2. Synthesis of the nucleosides antibiotic nucleocidine. *Journal of the American Chemical Society* **98**:3346–3357.

Johnson CR, Esker JL & Van Zandt MC (1994) Chemoenzymatic synthesis of 4-substituted riboses. S-(4′-methyladenosyl)-L-homocysteine. *Journal of Organic Chemistry* **59**:5854–5855.

Jones GH, Taniguchi M, Tegg D & Moffatt JG (1979) 4′-Substituted nucleosides. 4. Synthesis of some 4′-hydroxymethyl nucleosides. *Journal of Organic Chemistry* **44**:1309–1317.

Jung ME & Toyota A (2001) Preparation of 4′-substituted thymidines by substitution of the thymidine 5′-esters. *Journal of Organic Chemistry* **66**:2624–2635.

Kato K, Suzuki H, Tanaka H & Miyasaka T (1998) Enantio- and diastereoselective synthesis of 4′-a-substituted carbocyclic nucleosides. *Tetrahedron: Asymmetry* **9**:911–914.

Kitano K, Machida H, Miura S & Ohrui H (1999) Synthesis of novel 4′-*C*-methyl-pyrimidine nucleosides and their biological activities. *Bioorganic & Medicinal Chemistry Letters* **9**:827–830.

Kitano K, Miura S, Ohrui H & Meguro H (1997) Synthesis of 4′-*C*-fluoromethylnucleosides as potential antineoplastic agents. *Tetrahedron* **53**:13315–13322.

Kodama E, Kohgo S, Kitano K, Machida H, Gatanaga H, Shigeta S, Matsuoka M, Ohrui H & Mitsuya H (2001) 4′-Ethynyl nucleoside analogs: potent inhibitors of multidrug-resistant human immunodeficiency virus variants *in vitro*. *Antimicrobial Agents & Chemotherapy* **45**:1539–1546.

Kohgo S, Horie H & Ohrui H (1999) Synthesis of 4′-*C*-ethynyl-β-D-*arabino*- and 4′-*C*-ethynyL-2′-deoxy-β-D-ribo-pentofuranosyl pyrimidines, and their biological evaluation. *Bioscience Biotechnology & Biochemistry* **63**:1146–1149.

Kohgo S, Kodama E, Shigeta S, Saneyoshi M, Machida H & Ohrui H (1999) Synthesis of 4′-substituted nucleosides and their biological evaluation. *Nucleic Acids Symposium Series* **42**:127–128.

Kohgo S, Mitsuya H & Ohrui H (2001) Synthesis of the L-enantiomer 4′-*C*-ethynyl-2′-deoxycytidine. *Bioscience Biotechnology & Biochemistry* **65**:1879–1882.

Kozak J & Johnson CR (1998) Synthesis of 4′-trifluoromethyl nucleoside analogs. *Nucleosides & Nucleotides* **17**:2221–2239.

Maag H, Rydzewski RM, McRoberts MJ, Crawford-Ruth D, Verheyden JPH & Prisbe EJ (1992) Synthesis and anti-HIV activity of 4′-azido- and 4′-methoxynucleosides. *Journal of Medicinal Chemistry* **35**:1440–1451.

Marx A, Erdmann P, Senn M, Körner S, Jungo T, Petretta M, Imwinkelried P, Dussy A, Kulicke KJ, Macko L, Zehnder M & Giese B (1996) Synthesis of 4′-*C*-acylated thymidines. *Helvetica Chimica Acta* **79**:1980–1994.

Murakami K, Shirasaka T, Yoshioka H, Kojima E, Aoki S, Ford Jr. H, Driscoll JS, Kelley JA & Mitsuya H (1991) *Escherichia coli* mediated biosynthesis and *in vitro* anti-HIV activity of lipophilic 6-halo-2′,3′-dideoxypurine nucleosides. *Journal of Medicinal Chemistry* **34**:1606–1612.

Nomura M, Shuto S, Tanaka M, Sasaki T, Mori S, Shigeta S & Matsuda A (1999) Nucleosides & Nucleotides 185. Synthesis and biological activities of 4′α-*C*-branched-chain sugar pyrimidine nucleosides. *Journal of Medicinal Chemistry* **42**:2901–2908.

O-Yang C, Kurz W, Eugui EM, McRoberts MJ, Verheyden JPH, Kurz LJ & Walker KAM (1992) 4′-Substituted nucleosides as inhibitors of HIV: an unusual oxetane derivative. *Tetrahedron Letters* **33**:41–44.

O-Yang C, Wu HY, Fraser-Smith EB & Walker KAM (1992) Synthesis of 4′-cyanothymidine and analogs as potent inhibitors of HIV. *Tetrahedron Letters* **33**:37–40.

Ohrui H, Kohgo S, Kitano K, Sakata S, Kodama E, Yoshimura K, Matsuoka M, Shigeta S & Mitsuya H (2000) Syntheses of 4′-*C*-ethynyl-β-D-*arabino*- and 4′-*C*-ethynyl-2′-deoxy-β-D-ribo-pentofuranosylpyrimidines and -purines and evaluation of their anti-HIV activity. *Journal of Medicinal Chemistry* **43**:4516–4525.

Ohrui H & Mitsuya H (2001) 4′-*C*-Substituted-2′-deoxynucleosides: a family of retroviral agents which are potent against drug-resistant HIV variants. *Current Drug Targets–Infectious Disorders* **1**:1–10.

Ohrui H, Nishizaki T, Waga T & Meguro H (1991) Synthetic study on 4′-*C*-methylnucleosides: Part I, synthesis of 4-*C*-methyl-D-ribofuranose derivative. *Nucleic Acids Symposium Series* **25**:1–2.

Owen GR, Verheyden, JPH & Moffatt JG (1976) 4′-Substituted nucleosides. 3. Synthesis of some 4′-fluorouridine derivatives. *Journal of Organic Chemistry* **41**:1310–1317.

Prisbe EJ, Maag H, Verheyden JPH & Rydzewski RM (1993) Structure–activity relationships among HIV inhibitory 4′-substituted nucleosides. *Nucleosides & Nucleotides as Antitumor & Antiviral Agents*. Edited by CK Chu & DC Baker. New York: Plenum Press, pp. 101–113.

Secrist III JA & Winter Jr WJ (1978) Carbon-carbon bond formation at C_4' of a nucleoside. Synthesis and utilization of a uridine 4′, 5′-enamine. *Journal of the American Chemical Society* **100**:2554–2555.

Singh SK, Kumar R & Wengel J (1998) Synthesis of novel bicyclo[2.2.1]ribonucleosides: 2′-amino- and 2′-thio-LNA monomeric nucleosides. *Journal of Organic Chemistry* **63**:6078–6079.

Sugimoto I, Shuto S, Mori S, Shigeta S & Matsuda A (1999) Nucleosides & Nucleotides 183. Synthesis of 4′α-branched thymidines as a new type of antiviral agent. *Bioorganic & Medicinal Chemistry Letters* **9**:385–388.

Summerer D & Marx A (2001) DNA polymerase selectivity: sugar interactions monitored with high-fidelity nucleotides. *Angewandte Chemie International Edition* **40**:3693–3695.

Thrane H, Fensholdt J, Renger M & Wengel J (1995) Novel linear and branched oligodeoxynucleotide analogues containing 4′-*C*-(hydroxymethyl)thymidine. *Tetrahedron* **51**:10389–10402.

Verheyden, JPH & Moffatt JG. (1975) 4′-Substituted nucleosides, 1. Synthesis of 4′-methoxyuridine and related compounds. *Journal of the American Chemical Society* **97**:4386–4395.

Waga T, Nishizaki T, Miyakawa I, Ohrui H & Meguro H (1993) Synthesis of 4′-*C*-methylnucleosides. *Bioscience Biotechnology Biochemistry* **57**:1433–1438.

Waga T, Ohrui H & Meguro H (1996) Synthesis and biological evaluation of 4′-*C*-methylnucleosides. *Nucleosides & Nucleotides* **15**:287–304.

Wang G, Middleton PJ, Lin C & Pietrzkowski Z (1999) Biophysical and biochemical properties of oligodeoxynucleotides containing 4′-*C*- and 5′-*C*-substituted thymidines. *Bioorganic & Medicinal Chemistry Letters* **9**:885–890.

Wang G & Seifert WE (1996) Synthesis and evaluation of oligodeoxynucleotides containing 4′-*C*-substituted thymidines. *Tetrahedron Letters* **37**:6515–6518.

Yamaguchi T, Tomikawa A, Hirai T, Kawaguchi T, Ohrui H & Saneyoshi M (1997) *Nucleosides & Nucleotides* **16**:1347–1350.

Youssefyeh R, Tegg D, Verheyden, JPH, Jones GH & Moffatt JG (1977) Synthetic routes to 4′-hydroxymethylnucleosides. *Tetrahedron Letters* **18**:435–438.

Youssefyeh RD, Verheyden, JPH & Moffatt JG (1979) 4′-Substituted nucleosides. 4. Synthesis of some 4′-hydroxymethyl nucleosides. *Journal of Organic Chemistry* **44**:1301–1308.

Received 5 January 2004; accepted 31 March 2004

Structure−Activity Relationships of Cyclic Peptide-Based Chemokine Receptor CXCR4 Antagonists: Disclosing the Importance of Side-Chain and Backbone Functionalities

Satoshi Ueda,[†] Shinya Oishi,[†] Zi-xuan Wang,[‡] Takanobu Araki,[†] Hirokazu Tamamura,[†,#] Jérôme Cluzeau,[†] Hiroaki Ohno,[†] Shuichi Kusano,[∥] Hideki Nakashima,[∥] John O. Trent,[§] Stephen C. Peiper,[‡] and Nobutaka Fujii[†,*]

Graduate School of Pharmaceutical Sciences, Kyoto University, Sakyo-ku, Kyoto 606-8501, Japan, Department of Pathology, Medical College of Georgia, Georgia 30912, Institute of Biomaterials and Bioengineering, Tokyo Medical and Dental University, Chiyoda-ku Tokyo 101-0062, Japan, St. Marianna University, School of Medicine, Miyamae-ku, Kawasaki 216-8511, Japan, and James Graham Brown Cancer Center, University of Louisville, Kentucky 40202

Received June 19, 2006

Previously, we have identified a highly potent CXCR4 antagonist **2** [cyclo(-D-Tyr[1]-Arg[2]-Arg[3]-Nal[4]-Gly[5]-)] and its Arg[2] epimer **3** [cyclo(-D-Tyr[1]-D-Arg[2]-Arg[3]-Nal[4]-Gly[5]-)] by the screening of cyclic pentapeptide libraries that were designed based on the structure−activity relationship studies on 14-residue peptidic CXCR4 antagonist **1**. In the present study, a new series of analogues of **2** and **3** were synthesized to evaluate the influences of peptide side-chain and backbone modification on bioactivities. Based on the Ala-scanning study, in which each residue in **2** and **3** was replaced with Ala having the identical chirality, substitution of Arg[3] and Nal[4] [Nal = L-3-(2-naphthyl)alanine] with Ala (compounds **6**, **7**, **10**, **11**) led to significant loss of the potency, indicating these amino acids are more important contributors to the bioactivity. For the cyclic peptide backbone, several modifications including D/L-Ala or cyclic amino acids substitution at the Gly[5] position and sequential *N*-methylation on amide nitrogens were conducted. Among the analogues, compounds **13** [cyclo(-D-Tyr[1]-Arg[2]-Arg[3]-Nal[4]-D-Ala[5]-)] and **32** [cyclo(-D-Tyr[1]-D-MeArg[2]-Arg[3]-Nal[4]-Gly[5]-)] were close in potency to the most potent lead **2**. NMR and conformational analysis indicated that both of these analogues favor the same backbone conformation as **2**, whereas similar analysis of less potent analogues indicates that an altered backbone conformation is favored. The conformational analysis showed that steric repulsion by a 1,3-allylic strain-like effect across the planar peptide bond might contribute to the conformational preferences of cyclic pentapeptides.

Introduction

Chemokines comprise a protein family of chemotactic factors that bind G protein-coupled receptors.[1,2] Engagement of chemokine receptors by their ligands triggers changes of the receptor conformation that lead to the initiation of a signaling cascade involving G protein binding, protein kinase activation, Ca^{2+} mobilization from intracellular stores, and cytoskeletal rearrangement, eventually leading to directed cell migration toward the gradients of the respective ligand.[3,4] A chemokine receptor CXCR4 and its endogenous ligand CXCL12 (stromal cell derived factor-1, SDF-1) are partners in multiple important functions in normal physiology involving the leukocyte chemotaxis in the immune system[5] and progenitor cell migration during embryologic development of the cardiovascular,[6,7] hemopoietic,[8] and central nervous systems.[9,10] On the other hand, CXCR4 has also multiple functions in pathologic physiology. CXCR4 serves as a coreceptor for infection of T cell line-tropic (X4) strains of the human immunodeficiency virus type 1 (HIV-1[a]). Following activation of the gp120 subunits of the envelope glycoprotein by binding to CD4, CXCR4 leads to membrane fusion and subsequent entry of the viral genome into the target cell.[11,12] Recently, Müller et al. disclosed that CXCL12/CXCR4 interactions participate in breast cancer metastasis analogous to programming directed migration in normal leukocytes and progenitor cells.[13] Expression of CXCR4 is enriched on the surface of malignant primary breast cancer cells while CXCL12 is preferentially expressed in organs that are frequent sites of metastasis in breast cancer, such as lung, liver, lymph nodes, and bone marrow. The coordinate actions between an attractant molecule and the corresponding receptor allow tumor cells to spread specifically to distant organs that provide a supportive niche. Furthermore, Nanki et al. reported that CXCL12/CXCR4 interactions might play a central role in memory T cell migration into inflamed rheumatoid arthritis (RA) synovium and for persisting inflammation at the affected site mediated by $CD4^+$ T cells.[14]

Thus, CXCR4 is considered as an important therapeutic target for multiple diseases. Several potent CXCR4 antagonists have been developed so far. Among them, a β-sheet-like 14-residue peptide **1** was identified by potency optimization of a 18-residue cyclic peptide isolated from horseshoe crabs (Figure 1).[15] The peptide **1** and its analogues were also characterized as HIV-1 entry inhibitors,[16] anticancer-metastatic,[17,18] and anti-RA agents.[19] Several other low-molecular-weight CXCR4 antagonists such as AMD3100[20,21] and KRH1636[22] have also been reported to inhibit HIV-1 infection through CXCR4. Recently, we have identified novel potent CXCR4 antagonists **2** and **3** by screening of two orthogonal cyclic pentapeptide libraries,[23] which were designed based on the structure−activity relationship studies on **1** (Figure 1).[24] These peptides contain two arginine, one 3-(2-naphthyl)alanine, and one tyrosine residue, that potentially

* Corresponding author. Tel: +81-75-753-4551, Fax: +81-75-753-4570, E-mail: nfujii@pharm.kyoto-u.ac.jp
† Kyoto University.
‡ Medical College of Georgia.
# Tokyo Medical and Dental University.
∥ St. Marianna University.
§ University of Louisville.

[a] Abbreviations: Nal, L-3-(2-naphthyl)alanine; Pic, pipecolic acid; Sar, sarcosine; HIV-1, human immunodeficiency virus type 1; RA, rheumatoid arthritis; SA-MD, simulated annealing molecular dynamics; AMD3100, 1,1′-[1,4-phenylenebis(methylene)]-bis(1,4,8,11-tetraazacyclotetradecane); KRH1636, *N*-{(*S*)-4-guanidino-1-[(*S*)-1-naphthalen-1-yl-ethylcarbamoyl]butyl}-4-{[(pyridin-2-yl-methyl)amino]methyl}benzamide.

10.1021/jm0607350 CCC: $37.00
Published on Web 12/29/2006

Scheme 1[a]

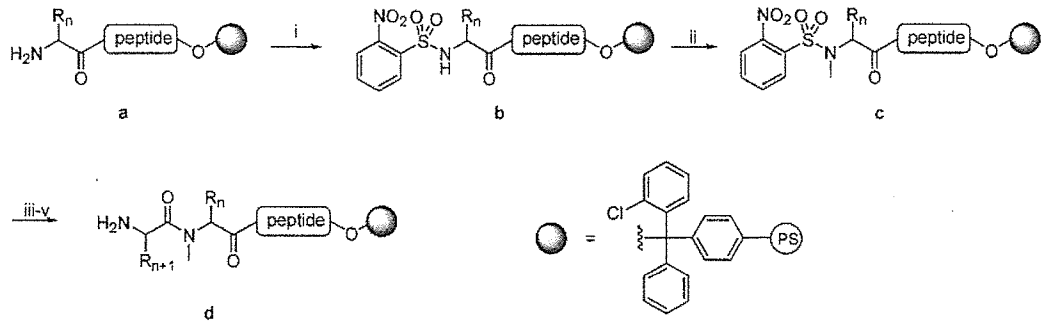

[a] Reagents: (i) *o*-nitrobenzenesulfonyl chloride, 2,4,6-collidine; (ii) MeOH, PPh_3, DEAD; (iii) DBU, 2-mercaptoethanol; (iv) Fmoc-AA-OH, HATU, HOAT, DIPEA; (v) piperidine.

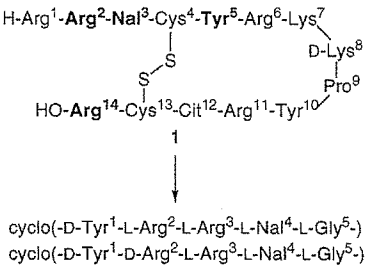

Figure 1. Structures of **1** and its downsized peptides **2** and **3**. Bold residues are the indispensable residues of **1** for the potent CXCR4-antagonistic activity. Nal = L-3-(2-naphthyl)alanine, Cit = L-citrulline.

correspond to the pharmacophore residues of the parent peptide **1**. We[25–27] and others[28] have performed several modifications on **2** including incorporation of (*E*)-alkene or reduced-amide dipeptide isosteres and conformationally constrained amino acid analogues, and fine-tuning of backbone ring structures. However, systematic modifications of **2** to design more potent antagonists have not been reported so far. In order to clarify the elements among the peptide side-chain and backbone functional groups indispensable for the ligand binding to CXCR4, chemical derivatization of **2** and **3** was conducted. In this manuscript, we describe the details of structure–activity relationship studies on cyclic pentapeptide-based CXCR4 antagonists **2** and **3** as well as identification of a more potent CXCR4 antagonist.

Chemistry. Synthesis on solid support of all peptides was performed on 2-chlorotrityl [(2-Cl)Trt] resin in parallel using usual Fmoc-based solid-phase peptide synthesis as described in the Experimental Section. *t*-Bu and 2,2,4,6,7-pentamethyldihydrobenzofuran-5-sulfonyl (Pbf) groups were employed for Tyr and Arg residue side-chain protection, respectively. L-Ala, D-Ala, L-Pro, D-Pro, L-pipecolic acid (L-Pic), D-Pic, β-alanine (β-Ala), and L-Nal were employed for the C-terminal residues of **12/19**, **13/20**, **14/21**, **15/22**, **16/23**, **17/24**, **18/25**, and **26/31**, respectively. The Gly residue was positioned at the C-terminal of the other peptide resins to avoid potential epimerization during the cyclization. For the preparation of *N*-methyl amino acid-containing peptide resins, an *N*-methyl group was incorporated on the α-amino group by a site-selective method reported by Miller et al.[29,30] (Scheme 1). The α-amino group was temporarily protected with an *o*-nitrobenzenesulfonyl (*o*-Ns) group before *N*-methylation by the Mitsunobu reaction. After removal of the *o*-Ns group by treatment with 1,8-diazabicyclo[5.4.0]undec-7-ene (DBU) and 2-mercaptoethanol, the subsequent amino acids were coupled using *O*-(7-azabenzotriazol-1-yl)-1,1,3,3-tetramethyluronium hexafluorophosphate (HATU)[31] as an activating reagent. Treatment of protected peptide resins with 20% (v/v) 1,1,1,3,3,3-hexafluoroisopropanol (HFIP) in CH_2Cl_2[32] provided linear protected peptides, which were cyclized with diphenylphosphoryl azide (DPPA) in DMF. Final deprotection with TFA–H_2O (95:5) followed by reverse-phase HPLC purification afforded the cyclic peptides. All peptides were identified with ion-spray mass spectrometry, and the purity was more than 95% by analytical HPLC.

Table 1. Biological Activities of **2**, **3**, and the Ala-Substituted Derivatives

peptide	sequence[a]	IC_{50} (μM)[b]	EC_{50} (μM)[c]
2	cyclo(-D-Tyr-L-Arg-L-Arg-L-Nal-Gly-)	0.004	0.16
4	cyclo(-D-Ala-L-Arg-L-Arg-L-Nal-Gly-)	>1	115
5	cyclo(-D-Tyr-L-Ala-L-Arg-L-Nal-Gly-)	0.063	12
6	cyclo(-D-Tyr-L-Arg-L-Ala-L-Nal-Gly-)	>1	>120
7	cyclo(-D-Tyr-L-Arg-L-Arg-L-Ala-Gly-)	>1	>120
3	cyclo(-D-Tyr-D-Arg-L-Arg-L-Nal-Gly-)	0.008	0.39
8	cyclo(-D-Ala-D-Arg-L-Arg-L-Nal-Gly-)	0.13	29
9	cyclo(-D-Tyr-D-Ala-L-Arg-L-Nal-Gly-)	0.23	16
10	cyclo(-D-Tyr-D-Arg-L-Ala-L-Nal-Gly-)	>1	60
11	cyclo(-D-Tyr-D-Arg-L-Arg-L-Ala-Gly-)	>1	>120

[a] The substituted residues from the parent peptides **2** and **3** are designated by underlining. [b] IC_{50} values for the cyclic pentapeptides are based on inhibition of [^{125}I]SDF-1 binding to CXCR4 transfectants of CHO cells. [c] EC_{50} values are based on the inhibition of HIV-induced cytopathogenicity in MT-4 cells. All data are the mean values for at least three independent experiments.

Results and Discussion

Identification of Indispensable Pharmacophore Functionality by Alanine-Scanning. Our first attempt was to identify the minimal side-chain functional group requirement of **2** and **3** for CXCR4 antagonism. To evaluate the comparative significance of side-chain functionality, each residue except for the Gly residue of **2** and **3** was substituted with Ala. Because the chirality of Ala was identical to that of the corresponding residue in parent peptides, exhibition of similar conformations was expected even after the substitution. All Ala-substituted peptides **4**–**11** showed significantly less CXCR4 antagonistic and anti-HIV activities when compared to the parent peptides **2** and **3**. Ala^3- or Ala^4-substituted analogues **6**, **7**, **10**, and **11** did not show any CXCR4 antagonistic activity up to 1 μM (Table 1). This indicates that all the side-chain functional groups are important for the high CXCR4 antagonistic activity. On the other hand, L/D-Ala^2-substituted analogues, **5** and **9**, and D-Ala^1-substituted analogue **8** maintained moderate activities (**5**: IC_{50} = 63 nM, EC_{50} = 12 μM; **8**: IC_{50} = 130 nM, EC_{50} = 29 μM; **9**: IC_{50} = 230 nM, EC_{50} = 16 μM), although the potencies were less than one-twentieth of the parent peptides. These data suggest that the phenol group of D-Tyr^1 and a guanidino group of Arg^2 do not play a critical role in receptor binding, while guanidino group of Arg^3 and naphthalene group of Nal^4 are indispensable for the ligand interaction with CXCR4. This

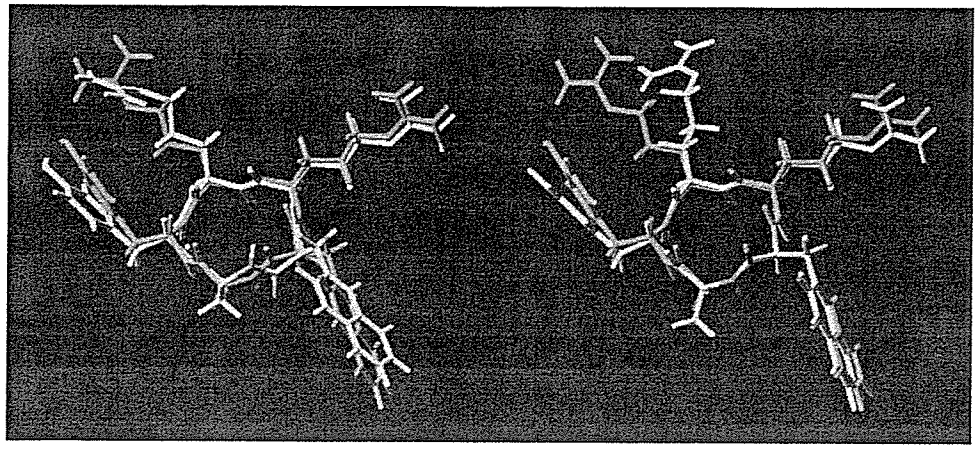

Figure 2. Superimposition of low-energy structures of **2** (purple) and **12** (green, left) or **13** (green, right).

propensity is consistent with the previous structure−activity relationship studies on **1**, where Ala-substitutions at the Arg^2-Nal^3 motif in **1** were more sensitive to anti-HIV activity as compared to the substitution of the other important residues, such as Tyr^5 and Arg^{14}.[24] It is noteworthy that two L/D-Ala^2-substituted peptides **5** and **9** having opposite chiralities retained moderate bioactivities. Recently, we have shown that L-Arg^2 in **2** could be replaced by nonbasic amino acids such as L-Phe-(4-F) (L-4-fluorophenylalanine) and D-MeAla without significant loss of CXCR4 antagonistic activity.[26,27] Hence, the functional group or the spatial disposition of the Arg^2 guanidino group could be further optimized.

Conformational Restriction of Cyclic Peptides by Modification of the Glycine Residue. In contrast to the finding that all side-chain functional groups of **2** and **3** were important for the high CXCR4 antagonistic activities, the Gly^5 position had many possibilities for further optimization. Since the absence of a side chain in Gly^5 possibly affected the conformational flexibility of the peptide backbone, it was expected that use of chiral or conformationally constrained amino acids would potentially restrict the global conformations to decrease the entropy losses upon the peptide binding on CXCR4. In order to evaluate the structure−activity relationship at the Gly^5 position, simple aliphatic amino acids were utilized for this study. In our previous conformational studies on **2**, characteristic orientations of the amide carbonyl groups of D-Tyr^1, Arg^2, Arg^3, and Gly^5 were observed in the low energy state.[23] These carbonyl oxygens were oriented away from the side chains of the respective following amino acids. This could be attributed to steric repulsion by a 1,3-allylic strain-like effect across the planar peptide bond.[33] On the other hand, the flexible Nal^4 ψ and Gly^5 ϕ angles had been expected, since there were two possibilities of Nal^4 carbonyl oxygen orientation. However, the carbonyl oxygen was directed away from the Gly^5 pro-*R* hydrogen atom in the calculated conformations, while the other orientation was not exhibited. This implied that the incorporation of a side chain having *R*-chirality (D-amino acid) at the Gly^5 position could restrict the rotation of the Nal^4-Gly^5 peptide bond plane. On the basis of this hypothesis, we introduced both enantiomers of Ala, Pro, and Pic to the Gly^5 position for conformational restriction. In addition, β-Ala was utilized for the optimization of carbon chain length at the Gly^5 position.

L-Ala^5-substituted analogues **12** and **19** showed less than 10-fold lower CXCR4 antagonistic and anti-HIV activities of the parent peptides **2** and **3**, respectively (Table 2, **12**: IC_{50} = 170 nM; EC_{50} = 20 μM, **19**: IC_{50} = 92 nM; EC_{50} = 10 μM). By contrast and as expected, more than 8-fold higher potencies were observed for D-Ala^5-substituted analogues **13** and **20** (**13**: IC_{50} = 11 nM; EC_{50} = 0.49 μM, **20**: IC_{50} = 11 nM; EC_{50} = 0.67 μM) as compared to the corresponding L-Ala^5-substituted peptides **12** and **19**, respectively. The bioactivities of D-Ala^5-substituted analogues were approximately half of the parent peptides **2** and **3**. This suggested that substitution with L-Ala^5 resulted in significant conformational change, while D-Ala^5 substitution kept the bioactive conformations of the parent peptides **2** and **3**. Simulated annealing molecular dynamics (SA-MD) analysis demonstrated that the backbone conformation of **13** was similar to that of **2** but different from that of **12** (Figure 2). Local conformations around Nal^4 and Gly^5/D-Ala^5 were very similar between **2** and **13** as expected, while the conformation of L-Ala^5-substituted analogues **12** differed particularly in the opposite orientation of the Nal^4 carbonyl oxygen. These calculated structures are consistent with the observed NOE data; in L-Ala^5-substituted peptide **13**, strong NOE between Nal^4 H^α and D-Ala^5 H^N indicates that these hydrogen atoms were oriented into the same direction. On the other hand, the observed weak NOE between Nal^4 H^α and L-Ala^5 H^N in peptide **12** indicates these hydrogen atoms were oriented into the opposite directions. The 1,3-pseudo allylic strain between the Nal^4 carbonyl oxygen and the α-methyl group of D/L-Ala^5 could result in these different conformational preferences between **12** and **13**. This

Table 2. Biological Activities of the Gly^5-Modified Analogues of **2** and **3**

peptide	sequence[a]	IC_{50} (μM)[b]	EC_{50} (μM)[c]
2	cyclo(-D-Tyr-L-Arg-L-Arg-L-Nal-Gly-)	0.004	0.16
12	cyclo(-D-Tyr-L-Arg-L-Arg-L-Nal-L-Ala-)	0.17	20
13	cyclo(-D-Tyr-L-Arg-L-Arg-L-Nal-D-Ala-)	0.011	0.49
14	cyclo(-D-Tyr-L-Arg-L-Arg-L-Nal-L-Pro-)	>1	-[d]
15	cyclo(-D-Tyr-L-Arg-L-Arg-L-Nal-D-Pro-)	>1	-[d]
16	cyclo(-D-Tyr-L-Arg-L-Arg-L-Nal-L-Pic-)	>1	-[d]
17	cyclo(-D-Tyr-L-Arg-L-Arg-L-Nal-D-Pic-)	>1	-[d]
18	cyclo(-D-Tyr-L-Arg-L-Arg-L-Nal-β-Ala-)	0.047	3.0
3	cyclo(-D-Tyr-D-Arg-L-Arg-L-Nal-Gly-)	0.008	0.37
19	cyclo(-D-Tyr-D-Arg-L-Arg-L-Nal-L-Ala-)	0.092	10
20	cyclo(-D-Tyr-D-Arg-L-Arg-L-Nal-D-Ala-)	0.011	0.67
21	cyclo(-D-Tyr-D-Arg-L-Arg-L-Nal-L-Pro-)	> 1	-[d]
22	cyclo(-D-Tyr-D-Arg-L-Arg-L-Nal-D-Pro-)	> 1	-[d]
23	cyclo(-D-Tyr-D-Arg-L-Arg-L-Nal-L-Pic-)	0.64	-[d]
24	cyclo(-D-Tyr-D-Arg-L-Arg-L-Nal-D-Pic-)	> 1	-[d]
25	cyclo(-D-Tyr-D-Arg-L-Arg-L-Nal-β-Ala-)	0.35	38

[a] The substituted residues from the parent peptide **2** and **3** are underlined. [b] IC_{50} values for the cyclic pentapeptides are based on inhibition of [^{125}I]SDF-1 binding to CXCR4 transfectants of CHO cells. [c] EC_{50} values are based on the inhibition of HIV-induced cytopathogenicity in MT-4 cells. [d] Not tested. All data are the mean values for at least three independent experiments.

Table 3. Biological Activities of *N*-Methyl Amino Acid-Containing Analogues of **2** and **3**

peptide	sequence[a]	IC_{50} (μM)[b]	EC_{50} (μM)[c]
2	cyclo(-D-Tyr-L-Arg-L-Arg-L-Nal-Gly-)	0.004	0.16
26	cyclo(-D-MeTyr-L-Arg-L-Arg-L-Nal-Gly-)	0.128	-[d]
27	cyclo(-D-Tyr-L-MeArg-L-Arg-L-Nal-Gly-)	0.023	1.399
28	cyclo(-D-Tyr-L-Arg-L-MeArg-L-Nal-Gly-)	0.099	9.534
29	cyclo(-D-Tyr-L-Arg-L-Arg-L-MeNal-Gly-)	0.250	-[d]
30	cyclo(-D-Tyr-L-Arg-L-Arg-L-Ala-Sar-)	0.167	-[d]
3	cyclo(-D-Tyr-D-Arg-L-Arg-L-Nal-Gly-)	0.008	0.39
31	cyclo(-D-MeTyr-D-Arg-L-Arg-L-Nal-Gly-)	0.157	-[d]
32	cyclo(-D-Tyr-D-MeArg-L-Arg-L-Nal-Gly-)	0.003	0.088
33	cyclo(-D-Tyr-D-Arg-L-MeArg-L-Nal-Gly-)	0.021	0.782
34	cyclo(-D-Tyr-D-Arg-L-Arg-L-MeNal-Gly-)	0.563	-[d]
35	cyclo(-D-Tyr-D-Arg-L-Arg-L-Nal-Sar-)	0.256	-[d]

[a] *N*-Methylated residues are underlined. [b] IC_{50} values for the cyclic pentapeptides are based on inhibition of [^{125}I]SDF-1 binding to CXCR4 transfectants of CHO cells. [c] EC_{50} values are based on the inhibition of HIV-induced cytopathogenicity in MT-4 cells. [d] Not tested. All data are the mean values for at least three independent experiments.

could explain the reason for the higher potencies of D-Ala[5]-substituted analogues. The above information could serve for the further optimization of the Gly[5] position using D-amino acids having side-chain functionality.

Our next approach was to restrict global conformations of peptides **2** and **3** using cyclic amino acids such as L/D-Pro and L/D-Pic. These amino acids can provide a fused ring structure of cyclic peptides consisting of small and large rings. It was expected that the limited ϕ angle flexibility of Pro and Pic could contribute to the global conformational restriction.[34] Covalent linkage between the amide nitrogen and the side chain could also produce a favorable orientation of the Nal[4] carbonyl oxygen. However, L/D-Pro[5]- and L/D-Pic[5]-substituted peptides **14**−**17**, **21**, **22**, and **24** did not show CXCR4 inhibitory activities with IC_{50} values lower than 1 μM. Even the most potent peptide **23** exhibited an IC_{50} of only 0.64 μM. This suggests that the presence of cyclic amino acids at this position is sterically or conformationally unfavorable for the peptide−CXCR4 interaction. We could also assume that an amide proton at this position is required for high activity. This was supported by the fact that peptides having a sarcosin (Sar) at the Gly[5] position possessed less than one-thirtieth CXCR4 antagonistic activity of the parent peptides (see the next section). β-Ala[5]-substituted analogues **18** and **25** showed lower CXCR4 antagonistic and anti-HIV activities (**18**: IC_{50} = 47 nM, EC_{50} = 3 μM; **25**: IC_{50} = 350 nM, EC_{50} = 38 μM), indicating that expansion of the backbone ring size (16-membered ring) at this position is not favorable. Recently, we showed that reduction in the size of the backbone ring using γ-Nal [4-amino-5-(2-naphthyl)pentanoic acid] or γ-(*E*)-Nal [(*E*)-4-amino-5-(2-naphthyl)pent-2-enoic acid] unit (14-membered ring) instead of Nal[4]-Gly[5] dipeptide resulted in moderate to significant loss of CXCR4 antagonistic activity.[27] These observations suggest the importance of Gly[5] as a spacer for appropriate spatial orientation of the CXCR4 antagonist pharmacophores.

Identification of a Novel Potent CXCR4 Antagonist through *N*-Methyl Amino Acid-Scanning of 2 and 3. *N*-Methylation of the peptide backbone has been shown to be a valuable method in structure−activity relationship studies on bioactive peptides.[35−37] Substitutions with *N*-methyl amino acids often cause an increase or decrease in potency and selectivity of peptide ligands, providing useful information on the bioactive conformation. Hence, every amide bond of **2** and **3** was replaced sequentially with the corresponding *N*-methylated amide, and the bioactivities of obtained peptides were evaluated (Table 3). Peptides **26**, **28**, **29**, and **30** derived from *N*-methyl amino acid-scanning of peptide **2** showed more than 25-fold less CXCR4 antagonistic activity as compared to the parent peptide **2**. *N*-Methylated analogues **31, 34**, and **35** also showed a significant decrease in CXCR4 antagonism as compared to the parent peptide **3**. Use of L-MeArg[3] in peptide **33** slightly decreased the activity. *N*-Methylation at the Nal[4] position caused a remarkable decrease in CXCR4 antagonistic activity (**29**: IC_{50} = 250 nM; **34**: IC_{50} = 563 nM), suggesting that *N*-methylation at the putative receptor-binding motif (Arg[3]-Nal[4]) is unfavorable probably due to the absence of an amide proton. Previously, we showed that replacement of the Arg[3]-Nal[4] motif with the corresponding (*E*)-alkene dipeptide isostere unit (L-Arg[3]-ψ[(*E*)-CH=CH]-L-Nal[4]) or a reduced amide isostere unit (L-Arg[3]-ψ-[CH_2−NH]-L-Nal[4]) caused a significant loss of CXCR4 antagonistic activity.[25] These observations also indicate the importance of the Arg[3]-Nal[4] amide bond in both functional and conformational aspects.

On the other hand, the L/D-MeArg[2]-substituded peptides **27** and **32** showed potent CXCR4 antagonistic and anti-HIV activities (**27**: IC_{50} = 23 nM, EC_{50} = 1.4 μM; **32**: IC_{50} = 3.0 nM, EC_{50} = 0.088 μM), indicating that *N*-methylation at Arg[2] is not critical to antagonist activity. Interestingly, the D-MeArg[2] substitution (**32**) led to approximately 2-fold increase of CXCR4 antagonistic activity and more than 40-fold anti-HIV activity as compared with **3**, and these activities were nearly equal to those of **2**. NMR and SA-MD calculations showed that major conformer of **32** exhibited a backbone conformation similar to **2** but different from the parent peptide **3**, particularly with respect to the orientation of D-Tyr[1] carbonyl oxygen (Figure 3).[38] This conformation was also supported by strong NOEs between [D-Arg[2] H^{α} and D-Arg[2] H^{NMe}] and [D-Arg[2] H^{NMe} and Arg[3] H^{N}] in **32** (the corresponding strong NOEs were not observed in the parent peptide **3**; see Supporting Information). It is possible that an unfavorable 1,3-pseudo-allylic strain-like effect between the *N*-methyl group of D-MeArg[2] and D-Tyr[1] side chain of **32** induced the flip of D-Tyr[1]-D-Arg[2] amide group upon *N*-methylation of D-Arg[2], resulting in the identical local conformation around the D-Tyr[1]-D-MeArg[2] dipeptide with the D-Tyr[1]-L-Arg[2] conformation of **2**. Previously, we have shown a similar local conformational change upon *N*-methylation at the same position in D-Ala[2]-substituted analogues of **2**; i.e. cyclo(-D-Tyr[1]-D-MeAla[2]-Arg[3]-Nal[4]-Gly[5]-) showed 5-fold higher CXCR4 antagonistic activity (IC_{50} = 42 nM) than the nonmethylated peptide, cyclo(-D-Tyr[1]-D-Ala[2]-Arg[3]-Nal[4]-Gly[5]-) **9**.[27] It is also noted that the lower bioactivities of peptide **27** compared to **2** could be explained by the potential flip of the D-Tyr[1]-L-MeArg[2] amide bond orientation by *N*-methylation. These data suggest that the amide proton of Arg[2] has little contribution to bioactivity, and the amide bond orientation between D-Tyr[1] and D-MeArg[2] in **32** may contribute to its enhanced biological function.

Conclusion

Our present Ala-scanning study has shown that all of the side-chain functional groups contribute to high CXCR4 antagonistic activity of peptides **2** and **3**. In particular, Arg[3] and Nal[4] were proven to be indispensable for CXCR4 antagonistic activity. We have also shown that L-Ala substitution for Gly[5] of **2** or **3** caused a remarkable decrease in CXCR4 antagonistic and anti-HIV activities, while D-Ala substitution retained activity. Conformational studies revealed that D-Ala-substituted analogue **13** adopted a backbone conformation similar to that of **2**, which allows the rationalization of the biological activity for these

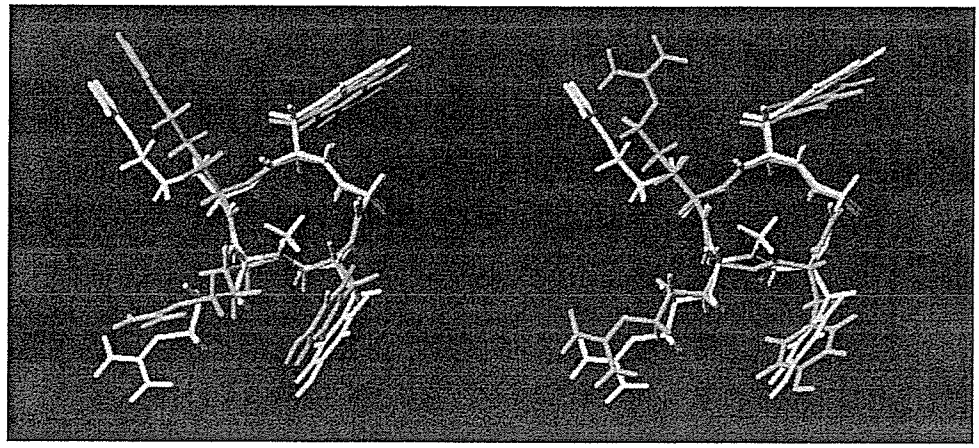

Figure 3. Superimposition of low-energy structures of **32** (green) and **2** (purple, left) or **3** (purple, right).

series of analogues. In addition, through comprehensive *N*-methyl-scanning of all residues in **2** and **3**, the *N*-methylated analogue **32** was characterized as one of the most potent cyclic pentapeptide-based CXCR4 antagonists synthesized thus far. The slight increase in CXCR4 antagonistic activity in **32** as compared to its nonmethylated analogue **3** could be explained by the favorable peptide bond orientation at the *N*-methylation site. Conformational studies suggested that the high potency in these series of compounds is due to the orientation of the backbone amide bonds, although direct interaction of the amide functions with the CXCR4 receptor is not clear. These results give valuable insight for understanding the ligand−receptor interactions and may also provide useful approaches for the design of new low-molecular-weight CXCR4 antagonists.

Experimental Section

General. Exact mass (HRMS) spectra were recorded on a JEOL JMS-01SG-2 or JMS-HX/HX 110A mass spectrometer. The ion-spray mass spectrum was obtained with a Sciex API*III*E triple quadrupole mass spectrometer (Toronto, Canada). Optical rotations were measured in water or 50% (v/v) water/AcOH solution with a Horiba high-sensitive polarimeter SEPA-200. ^{1}H NMR spectra were recorded using a Bruker AM 600 or JEOL JNM-ECA600 spectrometer at 600 MHz frequency, or JEOL JNM-AL400 spectrometer at 400 MHz frequency. Chemical shifts are calibrated to the solvent signal (2.49 ppm for DMSO, or 4.65 ppm for H_2O; s = singlet, d = doublet, dd = double doublet, m = multiplet). For HPLC separations, a Cosmosil 5C18-ARII analytical column (Nacalai Tesque, 4.6 × 250 mm, flow rate 1 mL/min) or a Cosmosil 5C18-ARII preparative column (Nacalai Tesque, 20 × 250 mm, flow rate 11 mL/min) was employed, and eluting products were detected by UV at 220 nm. A solvent system consisting of 0.1% TFA in water (v/v, solvent A) and 0.1% TFA in MeCN (v/v, solvent B) was used for HPLC elution.

Preparation of Amino Acid-Loaded 2-Chlorotrityl Resin. 2-Chlorotrityl chloride resin (1.25 mmol/g, 0.63 mmol) was treated with Fmoc-amino acid (0.69 mmol) and *N,N*-diisopropylethylamine (DIPEA) (2.77 mmol) in CH_2Cl_2 (5.00 mL) for 1.5 h. After the resin was washed with CH_2Cl_2, it was dried in vacuo. The loading was determined by measuring at 290 nm UV absorption of the piperidine-treated sample: Fmoc-L-Nal-(2-Cl)Trt-resin (0.72 mmol/g); Fmoc-L-Pro-(2-Cl)Trt-resin (0.78 mmol/g); Fmoc-D-Pro-(2-Cl)-Trt-resin (0.81 mmol/g); Fmoc-L-Pic-(2-Cl)Trt-resin (0.88 mmol/g); Fmoc-D-Pic-(2-Cl)Trt-resin (0.84 mmol/g); Fmoc-β-Ala-(2-Cl)Trt-resin (0.79 mmol/g).

Fmoc-Based Solid-Phase Peptide Synthesis. Protected peptide resins were manually constructed on a 0.10 mmol scale on H-L-Ala-(2-Cl)Trt-resin (0.89 mmol/g) for **12** and **19**, H-D-Ala-(2-Cl)-Trt-resin (0.90 mmol/g) for **13** and **20**, Fmoc-L-Pro-(2-Cl)Trt-resin for **14** and **21**, Fmoc-D-Pro-(2-Cl)Trt-resin for **15** and **22**, Fmoc-L-Pic-(2-Cl)Trt-resin for **16** and **23**, Fmoc-D-Pic-(2-Cl)Trt-resin for **17** and **24**, Fmoc-β-Ala-(2-Cl)Trt-resin for **18** and **25**, Fmoc-L-Nal-(2-Cl)Trt-resin for **26** and **31**, and H-Gly-Trt(2-Cl)Trt-resin (0.75 mmol/g) for the other peptides. Fmoc-amino acids were coupled using 1,3-diisopropylcarbodiimide (DIPCDI, 0.078 mL, 0.50 mmol) and *N*-hydroxybenzotriazole hydrate (HOBt·H_2O, 76 mg, 0.50 mmol) in DMF (1.0 mL) for 1.5 h. For the coupling of Fmoc-amino acid to the *N*-methyl amino acid, HATU (186 mg, 0.49 mmol) and 1-hydroxy-7-azabenzotriazole (HOAt, 68 mg, 0.50 mmol) were employed in place of DIPCDI/HOBt. The Fmoc group was deprotected by treatment with 20% (v/v) piperidine−DMF for 20 min.

***N*-Methyl Modification of *N*-Terminal α-Amino Group on Resin.** Resin (0.10 mmol) was treated with *o*-nitrobenzenesulfonyl chloride (66.5 mg, 0.30 mmol) and 2,4,6-collidine (0.066 mL, 0.50 mmol) in CH_2Cl_2 (1.0 mL) for 2 h at room temperature. After the resin was washed (CH_2Cl_2 × 3, DMF × 3, and THF × 3), to a suspension of the *N*-Ns-protected resin in anhydrous THF (1.0 mL) were added MeOH (0.020 mL, 0.50 mmol), PPh_3 (131 mg, 0.50 mmol), and diethyl diazodicarboxylate (0.227 mL, 0.50 mmol) at 0 °C. The mixture was shaken for 2 h at room temperature, followed by washing the resin (THF × 3 and $CHCl_3$ × 3). The *N*-methylated resin was treated with DBU (0.075 mL, 0.50 mmol) and 2-mercaptoethanol (0.070 mL, 1.0 mmol) for 1.5 h at room temperature to give the protected peptide resin having an *N*-methyl amino acid at the *N*-terminus.

Cleavage of Protected Peptides from the Resin and Cyclization. Protected peptide resin was treated with 20% (v/v) HFIP−CH_2Cl_2 (10 mL) for 2 h. After filtration of the resin, the filtrate was concentrated to provide the crude linear protected peptide. To the solution of the residue in DMF (30 mL) were added DPPA (0.539 mL, 0.25 mmol) and $NaHCO_3$ (42.0 mg, 0.50 mmol) at −40 °C. After being stirred for 36 h at room temperature, the whole was filtered, and the filtrate was concentrated to give the protected cyclic peptide, which was subjected to solid-phase extraction (SPE) over basic alumina in $CHCl_3$−MeOH (9:1) to remove inorganic salts derived from DPPA.

Deprotection of Protected Cyclic Peptide and HPLC purification. Protected cyclic peptides were treated with 95% (v/v) TFA solution (10 mL) for 2 h at room temperature. Concentration under reduced pressure and purification by preparative HPLC gave cyclic peptides.

Cell Culture. Human T-cell lines, MT-4 and MOLT-4 cells were grown in RPMI 1640 medium containing 10% heat-inactivated fetal calf serum, 100 IU/mL penicillin, and 100 μg/ mL streptomycin.

Virus. A strain of X4-HIV-1, HIV-1IIIB, was used for the anti-HIV assay. This virus was obtained from the culture supernatant of HIV-1 persistently infected MOLT-4/HIVIIIB cells and stored at −80 °C until used.

Anti-HIV-1 Assay. Anti-HIV-1 activity was determined based on the protection against HIV-1-induced cytopathogenicity in MT-4

cells. Various concentrations of test compounds were added to HIV-1 infected MT-4 cells at multiplicity of infection (MOI) of 0.01 and placed in wells of a flat-bottomed microtiter tray (1.5×10^4 cells/ well). After 5 days incubation at 37 °C in a CO_2 incubator, the number of viable cells was determined using the 3-(4,5-dimethylthiazol-2-yl)-2,5-diphenyltetrazolium bromide (MTT).

[^{125}I]-SDF-1 Binding and Displacement. Stable CHO cell transfectants expressing CXCR4 variant were prepared as describe previously.[39] CHO transfectants were harvested by treatment with trypsin−EDTA, allowed to recover in complete growth medium (MEM-α, 100 μg/ mL penicillin, 100 μg/mL streptomycin, 0.25 μg/mL amphotericin B, 10% (v/v)) for 4−5 h, and then washed in cold binding buffer (PBS containing 2 mg/mL BSA). For ligand binding, the cells were resuspended in binding buffer at 1×10^7 cell/mL, and 100 μL aliquots were incubated with 0.1 nM of [^{125}I]-SDF-1 (Perkin-Elmer Life Sciences) for 2 h on ice under constant agitation. Free and bound radioactivities were separated by centrifugation of the cells through an oil cushion, and bound radioactivity was measured with gamma-counter (Cobra, Packard, Downers Grove, IL). Inhibitory activity of test compounds was determined based on the inhibition of [^{125}I]-SDF-1 binding to CXCR4 transfectants (IC_{50}).

NMR Spectroscopy. The peptide sample was dissolved in DMSO-d_6 at a concentration of 5 mM. ^{1}H NMR spectra of the peptides were recorded at 300 K. The assignment of the proton resonance was achieved by use of ^{1}H−^{1}H COSY spectra. $^3J(H^N, H^\alpha)$ coupling constants were measured from one-dimensional spectra. The mixing time for NOESY experiments was set at 200 ms. NOESY spectra were composed of 512 real points in the F2 dimension and 256 real points, which were zero-filled to 256 points in the F1 dimension, with 144 scans per t1 increment. The cross-peak intensities were evaluated by relative build-up rates of the cross-peaks. **2**, **3**, **12**, and **13** exhibited one set of signals in ^{1}H NMR spectra. On the other hand, two distinct sets of signals were observed in ^{1}H NMR spectra of **32** with relative populations of 69% and 31%, indicating the existence of two conformations. For the minor conformer, NOESY spectra showed the NOE contact between α protons of D-Tyr^1 and D-MeArg^2 which is characteristic of the amide bond in a *cis* conformation. The major conformer did not exhibit any sequential H^α−H^α NOEs, suggesting this conformer adopt an all-*trans* conformation. The calculated structures of major and minor conformers exhibited *trans*- and *cis*-D-Tyr^1-D-MeArg^2 amide bond, respectively, which was consistent with the observed NOEs.

Calculation of Structures. The structure calculations were performed on a Silicon Graphics Origin 2000 workstation with the NMR refine program within the Insight II/Discover package using the consistent valence force field (CVFF). Pseudoatoms were defined for the CH_3^α protons of L-Ala^5 of **12**, D-Ala^5 of **13**, and *N*-methyl protons of **32**, and for all methylene protons of Nal^4, D-Tyr^1, D/L-Arg^2, and Arg^3, prochirality of which were not identified from ^{1}H NMR data. The dihedral ϕ angle constraints were calculated based on the Karplus equation: $^3J(H^N, H^\alpha) = 6.7\cos^2(\theta - 60°) - 1.3\cos(\theta - 60°) + 1.5$. Lower and upper angle errors were set to 15°. The NOESY spectrum with a mixing time of 200 ms was used for the estimation of the distances restraints between protons. The NOE intensities were classified into three categories (strong, medium, and weak) based on the number of contour lines in the cross-peaks to define the upper-limit distance restraints (1.7, 3.5, and 5.0 Å, respectively). The upper-limit restraints were increased by 1.0 Å for the involved pseudoatoms. Lower bounds between nonbonded atoms were set to their van der Waals radii (1.8 Å). These distance and dihedral angle restraints were included with force constants of 25−100 kcal/mol·Å^2 and 25−100 kcal/mol·rad^2, respectively. The 50 initial structures generated by the NMR refine program randomly were subjected to the simulated annealing calculations. The final minimization stage was achieved until the maximum derivative became less than 0.01 kcal/mol·Å^2 by the steepest descents and conjugate gradients methods. Excellent convergence was seen in the backbone structure of all calculated structures. The root-mean-square deviation (rmsd) values for all backbone structures of ten low-energy structures were below 0.23 Å.

Acknowledgment. This work was supported by Grant-in-Aid for Scientific Research from the Ministry of Education, Culture, Sports, Science, and Technology of Japan, and Health and Labour Sciences Research Grants (Research on HIV/AIDS) and Philip Morris USA Inc. and Philip Morris International. Computation time was provided by the Supercomputer Laboratory, Institute for Chemical Research, Kyoto University. S.U. and S.O. are grateful for the JSPS Research Fellowships for Young Scientists.

Supporting Information Available: Characterization data for all new compounds, ^{1}H NMR data of **2**, **3**, **12**, **13**, and **32**, and HPLC charts of representative compounds. This material is available free of charge via the Internet at http://pubs.acs.org.

References

(1) Murphy, P. M.; Baggiolini, M.; Charo I. F.; Herbert, C. A.; Horuk, R.; Matsushima, K.; Miller, L. H.; Oppenheim, J. J.; Power,.C. A. International union of pharmacology. XXII. Nomenclature for chemokine receptors. *Pharmacol. Rev.* **2000**, *52*, 145−176.
(2) Mackay, C. R.; Chemokines: immunology's high impact factors. *Nat. Immunol.* **2001**, *2*, 95−101.
(3) Premack, B. A.; Schall, T. J. Chemokine receptors: gateways to inflammation and infection. *Nat. Med.* **1996**, *2*, 1174−1178.
(4) Zlotnik, K.; Yoshie, O. Chemokines: a new classification system and their role in immunity. *Immunity* **2000**, *12*, 121−127.
(5) Bleul, C. C.; Fuhlbrigge, R. C.; Casanovas, J. M.; Aiuti, A.; Springer, T. A. A highly efficacious lymphocyte chemoattractant, stromal cell-derived factor 1 (SDF-1). *J. Exp. Med.* **1996**, *2*, 1101−1109.
(6) Tachibana, K.; Hirota, S.; Iizasa, H.; Yoshida, H.; Kawabata, K.; Kataoka, Y.; Kitamura, Y.; Matsushima, K.; Yoshida, N.; Nishikawa, S.; Kishimoto, T.; Nagasawa, T. The chemokine receptor CXCR4 is essential for vascularization of the gastrointestinal tract. *Nature* **1998**, *393*, 591−594.
(7) Nagasawa, T.; Hirota, S.; Tachibana, K.; Takakura, N.; Nishikawa, S.; Kitamura, Y.; Yoshida, N.; Kikutani, H.; Kishimoto, T. Defects of B-cell limphopoiesis and bone-marrow myelopoiesis in mice lacking the CXC chemokine PBSF/SDF-1. *Nature* **1996**, *382*, 635−638.
(8) Aiuti, A.; Webb, I. J.; Bleul, C.; Springer, T.; Gutierrez-Ramos, J. C. The chemokine SDF-1 is a chemoattractant for human CD34$^+$ hematopoietic progenitor cells and provides a new mechanism to explain the mobilization of CD34$^+$ progenitors to peripheral blood. *J. Exp. Med.* **1997**, *2*, 111−120.
(9) Zhu, Y.; Yu, Y.; Zhang, X. C.; Nagasawa, T.; Wu, J. Y.; Rao, Y. Role of the chemokine SDF-1 as the meningeal attractant for embryonic cerebellar neurons. *Nat. Neurosci.* **2002**, *5*, 719−720.
(10) Stumm, R. K.; Zhou, C.; Ara, T.; Lazarini, F.; Dubois-Dalcq, M.; Nagasawa, T.; Hollt, V.; Schulz, S. CXCR4 regulates interneuron migration in the developing neocortex. *J. Neurosci.* **2003**, *23*, 5123−5130.
(11) Feng, Y.; Broder, C. C.; Kennedy, P. E.; Berger, E. A. HIV-1 entry co-factor: Functional cDNA cloning of a seven-transmembrane G protein-coupled receptor. *Science* **1996**, *272*, 872−877.
(12) Oberlin, E.; Amara, A.; Bachelerie, F.; Bessia, C.; Virelizier, J. L.; Arenzana-Seisdedos, F.; Schwartz, O.; Heard, J. M.; Clark-Lewis, I.; Legler, D. L.; Loetscher, M.; Baggiolini, M.; Moser, B. The CXC chemokine SDF-1 is the ligand for LESTR/fusin and prevents infection by T-cell-line-adapted HIV-1. *Nature* **1996**, *382*, 833−835.
(13) Müller, A.; Homey, B.; Soto, H.; Ge, N.; Catron, D.; Buchanan, M. E.; Mcclanahan, T.; Murphy, E.; Yuan, W.; Wagner, S. M.; Barrera, J. L.; Mohar, A.; Verástegui, E.; Zlotnik, A. Involvement of chemokine receptors in breast cancer metastasis. *Nature* **2001**, *410*, 50−56.
(14) Nanki, T.; Hayashida, K.; El-Gabalawy, H. S.; Suson, S.; Shi, K.; Girschick, H. J., Yavuz, S.; Lipsky, P. E. Stromal cell-derived factor-1-CXC chemokine receptor interactions play a central role in CD4$^+$ T cell accumulation in rheumatoid arthritis synovium. *J. Immunol.* **2000**, *165*, 6590−6598.
(15) Masuda, M.; Nakashima, H.; Ueda, T.; Naba, H.; Ikoma, R.; Otaka, A.; Terakawa, Y.; Tamamura, H.; Ibuka, T.; Murakami, T.; Koyanagi, Y.; Waki, M.; Matsumoto, A.; Yamamoto, N.; Funakoshi, S.; Fujii,

N. A novel anti-HIV synthetic peptide, T-22 ([$Tyr^{5,12}$,Lys^{7}]-polyphemusin II). *Biochem. Biophys. Res. Commun.* **1992**, 189, 845−850.
(16) Tamamura, H.; Xu, Y.; Hattori, T.; Zhang, X.; Arakaki, R.; Kanbara, K.; Omagari, A.; Otaka, A.; Ibuka, T.; Yamamoto, N.; Nakashima, H.; Fujii, N. A low molecular weight inhibitor against the chemokine redeptor CXCR4: a strong anti-HIV peptide T140. *Biochem. Biophys. Res. Commun.* **1998**, *253*, 877−882.
(17) Tamamura, H.; Hori, A.; Kanzaki, N.; Hiramatsu, K.; Mizumoto, M.; Nakashima, H.; Yamamoto, N.; Otaka, A.; Fujii, N. T140 analogues as CXCR4 antagonists identified as anti-metastatic agent in the treatment of breast cancer. *FEBS Lett.* **2003**, *550*, 79−83.
(18) Takenaga, M.; Tamamura, H.; Hiramatsu, K.; Nakamura, N.; Yamaguchi, Y.; Kitagawa, A.; Kawai, S.; Nakashima, H.; Fujii, N.; Igarashi, R. A single treatment with microcapsules containing a CXCR4 antagonist suppressed pulmonary metastasis of murine melanoma. *Biochem. Biophys. Res. Commun.* **2004**, 320, 226−232.
(19) Tamamura, H.; Fujisawa, M.; Hiramatsu, K.; Mizumoto, M.; Nakashima, H.; Yamamoto, N.; Otaka, A.; Fujii, N. Identification of a CXCR4 antagonist, T140 analog, as anti-rheumatoid arthritis agent. *FEBS Lett.* **2004**, *569*, 99−104.
(20) Schols, D.; Struyf, S.; Van Damme, J.; Este, J. A.; Henson, G.; De Clarcq, E. Inhibition of T-tropic HIV strains by selective antagonization of the chemokine receptor CXCR4. *J. Exp. Med.* **1997**, *186*, 1383−1388.
(21) Donzella, G. A.; Schols, D.; Lin, S. W.; Este, J. A.; Nagashima, K. A.; Maddon P. J. AMD3100, a small molecule inhibitor of HIV-1 entry via the CXCR4 co-receptor. *Nat. Med.* **1998**, *4*, 72−76.
(22) Ichiya, K.; Yokoyama-Kumakura, S.; Tanaka, Y.; Tanaka, R.; Hirose, K.; Bannai, K.; Edamatsu, T.; Yanaka, M.; Niitani, Y.; Miyano-Kurosaki, N.; Takaku, H.; Koyanagi, Y.; Yamamoto, N. A duodenally absorbable CXC chemokine receptor 4 antagonist, KRH-1636, exhibits a potent and selective anti-HIV-1 activity. *Proc. Natl. Acad. Sci. U.S.A.* **2003**, *100*, 4185−4190.
(23) Fujii, N.; Oishi, S.; Hiramatsu, K.; Araki, T.; Ueda, S.; Tamamura, H.; Otaka, A.; Kusano, S.; Terakubo, S.; Nakashima, H.; Broach, J. A.; Trent, J. O.; Wang, Z.; Peiper, S. C. Molecular-size reduction of a potent CXCR4-chemokine antagonist using orthogonal combination of conformation- and sequence-based libraries. *Angew. Chem. Int. Ed.* **2003**, *42*, 3251−3253.
(24) Tamamura, H.; Omagari, A.; Oishi, S.; Kanamoto, T.; Yamamoto, N.; Peiper, S. C.; Nakashima, H.; Otaka, A.; Fujii, N. Pharmacophore identification of a specific CXCR4 inhibitor, T140, lead to development of effective anti-HIV agents with very high selectivity indexes. *Bioorg. Med. Chem. Lett.* **2000**, *10*, 2633−2637.
(25) Tamamura, H.; Hiramatsu, K.; Ueda, S.; Wang, Z.; Kusano, S.; Terakubo, S.; Trent, J. O.; Peiper, S. C.; Yamamoto, N.; Nakashima, H.; Otaka, A.; Fujii, N. Stereoselective synthesis of [L-Arg-L/ D-3-(2-naphthyl)alanine]-type (*E*)-alkene dipeptide isosteres and its application to the synthesis and biological evaluation of pseudopeptide analogues of the CXCR4 antagonist FC131. *J. Med. Chem.* **2005**, *48*, 380−391.
(26) Tamamura, H.; Esaka, A.; Ogawa, T.; Araki, T.; Ueda, S.; Wang, Z.; Trent, J. O.; Tsutsumi, H.; Masuno, H.; Nakashima, H.; Yamamoto, N.; Peiper, S. C.; Otaka, A.; Fujii, N. Structure-activity relationship studies on CXCR4 antagonists having cyclic pentapeptide scaffolds. *Org. Biomol. Chem.* **2005**, *3*, 4392−4394.
(27) Tamamura, H.; Araki, T.; Ueda, S.; Wang, Z.; Oishi, S.; Esaka, A.; Trent, J. O.; Nakashima, H.; Yamamoto, N.; Peiper, S. C.; Otaka, A.; Fujii, N. Identification of novel low molecular weight CXCR4 antagonists by structural tuning of cyclic tetrapeptide scaffolds. *J. Med. Chem.* **2005**, *48*, 3280−3289.
(28) Marshall, G. R.; Wu, Y.; Heyden, N. V.; Ratner, L.; Nikiforovich, G. V. Backbone modification of cyclic pentapeptide antagonist of CXCR4. In *Peptides 2004 (Proceedings of 3rd international and 28th European peptide symposium)*; Flegel, M., Fridkin, M., Gilon, C., Slaninova, J., Eds.; Kenes International: Switzerland, 2005; pp 748−749.
(29) Miller, S. C.; Scanlan, T. S. Site-selective N-methylation of peptides on solid support. *J. Am. Chem. Soc.* **1997**, *119*, 2301−2302.
(30) Lin, X.; Dorr, H.; Nuss, J. M. Utilization of Fukuyama's sulfonamide protecting group for the synthesis of *N*-substituted α-amino acids and derivatives. *Tetrahedron Lett.* **2000**, *41*, 3309−3313.
(31) Carpino, L. A.; 1-Hydroxy-7-azabenzotriazole. An efficient peptide coupling additive. *J. Am. Chem. Soc.* **1993**, *115*, 4397−4398.
(32) Bollhagen, R.; Schmiedberger, M.; Barlos. K.; Grell. E. A new reagent for the cleavage of fully protected peptides synthesised on 2-chlorotrityl chloride resin. *J. Chem. Soc., Chem. Commun.* **1994**, 2559−2560.
(33) Haubner, R.; Finsinger, D.; Kessler, H. Stereoisomeric peptide libraries and peptidomimetics for designing selective inhibitors of the $\alpha_v\beta_3$ integrin for a new cancer therapy. *Angew. Chem. Int. Ed. Engl.* **1997**, *36*, 1374−1389.
(34) Toniolo, C. Conformationally restricted peptides through short range cyclization. *Int. J. Pept. Protein Res.* **1990**, *35*, 287−300.
(35) Dechantsreiter, M. A.; Planker, Eckart.; Matha, B.; Lohof, E.; Hölzemann, G.; Jonczyk, A.; Goodman, S. L.; Kessler, H. *N*-Methylated cyclic RGD peptides as highly active and selective $\alpha_v\beta_3$ integrin antagonists. *J. Med. Chem.* **1998**, *42*, 3033−3040.
(36) Rajeswaran, W. G.; Hocart, S. J.; Murphy, W. A.; Taylor, J. E.; Coy, D. H. Highly potent and subtype selective ligand derived by *N*-methyl scan of a somatostatin antagonist. *J. Med. Chem.* **2001**, *44*, 1305−1311.
(37) Erchegyi, J.; Hoeger, C. A.; Low, W.; Hoyer, D.; Waser, B.; Eltschinger, V.; Schaer, J.; Cescato, R.; Reubi, J. C.; Rivier, J. E. Somatostatin receptor 1 selective analogues: 2. N^{α}-Methylated Scan. *J. Med. Chem.* **2005**, *48*, 507−514.
(38) **32** exhibited two sets of signals in ^{1}H NMR spectra. The signals were assigned to *trans*- (69%) and *cis*- (31%) conformers at D-Tyr^1-D-$MeArg^2$ amide bond. Since backbone conformation and side chain disposition of *cis*-conformer of **32** was apparently different from the parent peptides **2** and **3**, we assumed that the major *trans*-conformer could contribute to the bioactivities of **32**, although contribution of the minor *cis*-conformer cannot be ruled out.
(39) Navenot, J. M.; Wang, Z. X.; Trent, J. O.; Murray, J. L.; Hu, Q. X.; DeLeeuw, L.; Moore, P. S.; Chang, Y.; Peiper, S. C. Molecular anatomy of CCR5 engagement by physiologic and viral chemokines and HIV-1 envelope glycoproteins; Differences in primary structural requirements for RANTES, MIP-1α, and vMIP-II binding. *J. Mol. Biol.* **2001**, *59*, 380−393.

JM0607350

A novel one-pot reaction involving organocopper-mediated reduction/transmetalation/asymmetric alkylation, leading to the diastereoselective synthesis of functionalized (*Z*)-fluoroalkene dipeptide isosteres†

Tetsuo Narumi,[a] Ayumu Niida,[a] Kenji Tomita,[a] Shinya Oishi,[a] Akira Otaka,[ab] Hiroaki Ohno[a] and Nobutaka Fujii*[a]

Received (in Cambridge, UK) 16th June 2006, Accepted 14th September 2006
First published as an Advance Article on the web 28th September 2006
DOI: 10.1039/b608596b

By a novel one-pot reaction sequence involving consecutive organocopper-mediated reduction, transmetalation and asymmetric alkylation, a highly diastereoselective synthesis of functionalized (*Z*)-fluoroalkene dipeptide isosteres was achieved in good to excellent yields.

Alkene-based dipeptide isosteres containing (*E*)-alkene or (*Z*)-fluoroalkene units are thought to be potential dipeptide mimetics.[1,2] (*Z*)-Fluoroalkene dipeptide isosteres are structurally similar to (*E*)-alkene dipeptide isosteres (EADIs), but differ in their electrostatic nature, which plays a significant role in their intra- and intermolecular interactions. Of note, due to the presence of the highly electronegative fluorine substituent, (*Z*)-fluoroalkene dipeptide isosteres more faithfully resemble native peptides than do EADIs. In this regard, there is increasing interest in the development of efficient methodologies for the stereoselective and divergent synthesis of (*Z*)-fluoroalkene isosteres.

The organocopper- or samarium diiodide (SmI_2)-mediated reduction of α,β-enoates, possessing leaving group(s) at the γ-position, is an effective methodology for the stereoselective synthesis of (*E*)-olefins and (*Z*)-fluoroolefins.[3,4] The dienolate intermediates resulting from the reduction can be efficiently trapped *in situ* by an appropriate electrophile, such as alkyl halides, aldehydes and ketones. Recently, we have applied this reduction/direct alkylation methodology to the synthesis of α-alkylated (*E*)-alkene and (*Z*)-fluoroalkene dipeptide isosteres (Fig. 1).[5,6] Although this reduction/direct alkylation of the difluoroenoate **1** is extremely useful for the regio- and stereoselective formation of the required (*Z*)-fluoroalkene unit, this synthetic route has not addressed the stereoselective construction of α-side chains. Since amino acids have a center of chirality, the equivalent side chains must be introduced with high stereoselectivity into the peptide isosteres. Herein, we report the diastereoselective synthesis of highly functionalized (*Z*)-fluoroalkene dipeptide isosteres by a novel one-pot reaction sequence, involving organocopper-mediated reduction, transmetalation and asymmetric alkylation as the key steps.

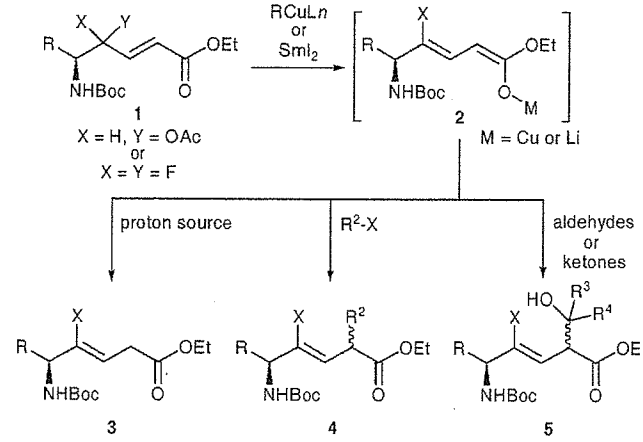

Fig. 1 Synthesis of (*E*)-alkene or (*Z*)-fluoroalkene dipeptide isosteres by a reduction/direct alkylation methodology.

The synthesis of the key intermediates, *N*-enoyl sultams **8** and **9**, is illustrated in Scheme 1. The α,α-difluoro-β-amino ester **7**[6] was reduced to an aldehyde and then subjected to Horner–Wadsworth–Emmons-type coupling with (*S*)- or (*R*)-*N*-diethoxyphosphonoacetylcamphorsultam[7] to give *N*-enoyl sultam **8** or **9** in an *E*-selective manner.

Initially, we examined the organocopper- and SmI_2-mediated reduction of **8**. Both reactions, using the Gilman reagent (Me_2CuLi·LiI·2LiBr at −78 °C for 30 min) and the cyano

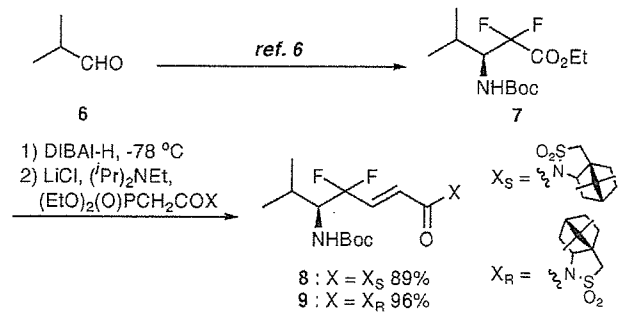

Scheme 1 Synthesis of the substrate for one-pot organocopper-mediated reduction/asymmetric alkylation.

[a]*Graduate School of Pharmaceutical Sciences, Kyoto University, Sakyo-ku, Kyoto 606-8501, Japan. E-mail: nfujii@pharm.kyoto-u.ac.jp*
[b]*Graduate School of Pharmaceutical Sciences, The University of Tokushima, Tokushima 770-8505, Japan*

† Electronic supplementary information (ESI) available: Experimental procedures, spectral data and analytical data for **12a**, and copies of ^1H and ^{13}C NMR spectra for all new compounds. See DOI: 10.1039/b608596b

Gilman reagent (Me_2CuLi·LiCN·2LiBr at −78 °C for 30 min), proceeded smoothly to yield the desired reduction product in 95 and 74% yields, respectively (Table 1, entries 1 and 2). Although the electron-donating ability of higher order cuprate (Me_3CuLi_2·LiI·3LiBr) is more effective than those of the Gilman and cyano Gilman reagents,[8] the reaction of **8** with higher order cuprate (Me_3CuLi_2·LiI·3LiBr at −78 °C for 30 min) afforded the reduction product in only a moderate yield (Table 1, entry 3). On the other hand, reaction with SmI_2,[9] which is well-recognized as a powerful one-electron reducing reagent,[10] afforded only a mixture of unidentified compounds (Table 1, entry 4). Based on these results, we chose the Gilman reagent as our reducing reagent.

Next, we carefully examined trapping of the dienolate intermediate with alkyl halides to construct the stereogenic center at the α-position. Initial attempts to trap the Cu or Li dienolates of intermediate **11a**, derived from **8** by organocopper-mediated reduction, with methyl iodide only furnished complex mixtures (Scheme 2). This prompted us to use the more reactive tin dienolate, which could be generated by the organocopper-mediated reduction of **8**, followed by treatment with triphenyltin chloride and HMPA.[11] Sequential reaction of **8** with Gilman reagent, triphenyltin chloride/HMPA and methyl iodide selectively afforded the α-methyl fluoroalkene isostere derivative (L-Val–ψ[(*Z*)-CF=CH]–L-Ala) (**12a**) in 93% isolated yield with exclusive *Z*-selectivity.‡ The diastereoselectivity of this reaction proved to be 80%, which was confirmed by RP-HPLC analysis.

In a similar manner, the use of benzyl bromide, *tert*-butyl bromoacetate and allyl bromide stereoselectively gave the corresponding α-substituted fluoroalkene dipeptide isosteres **12b**, **12c** and **12d**, respectively, in excellent yields (Table 2, entries 2 to 4). The reaction with methyl 3-bromopropionate gave the reduction product **10** with no alkylated product (Table 2, entry 5). Next, we attempted to synthesize epimeric (L,D)-type isosteres in a similar manner using (*R*)-sultam derivatives **9**. The reaction with Gilman reagent, followed by asymmetric alkylation *via* transmetalation, proceeded smoothly to afford the corresponding (L,D)-type α-substituted fluoroalkene isosteres **13a–13d** in high yields and with good to excellent diastereoselectivities (Table 2, entries 6 to 9).

Finally, the chiral auxiliary of **12b** was removed by hydrolysis under basic conditions to give the Boc–L-Val–ψ[(*Z*)-CF=CH]–L-Phe–OH isostere (**14**) in 75% yield with 96% de (Scheme 3). We observed neither epimerization of the α-alkyl groups nor isomerization of the double bond during cleavage of the chiral auxiliary.§

In conclusion, we have developed a novel and highly diastereoselective one-pot synthesis of functionalized (*Z*)-fluoroalkene dipeptide isosteres. The utility of the newly developed methodology can be found in the high-to-excellent regio- and stereoselectivities upon construction of the (*Z*)-fluoroalkene unit and α-side chain. Further studies using the developed methodology on the synthesis and evaluation of bioactive peptides with fluoroalkene isosteres are now in progress.

Table 1 Organocopper- and SmI_2-mediated reduction of *N*-enoyl sultam **8**

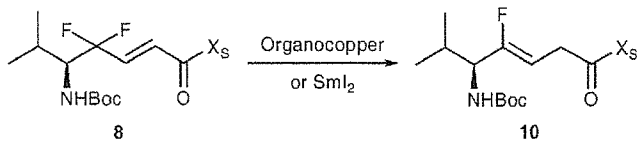

8 **10**

Entry	Reagent (equivalents)	Conditions	Yield[b] (%)
1	Me_2CuLi·LiI[a] (4)	−78 °C, 30 min	95
2	Me_2CuLi·LiCN[a] (4)	−78 °C, 30 min	74
3	Me_3CuLi_2·LiI[a] (4)	−78 °C, 30 min	52
4	SmI_2 (6)	0 °C, 30 min	—[c]

[a] In the presence of Li salts (LiCl and/or LiBr). [b] Isolated yield. [c] A mixture of unidentified compounds was obtained.

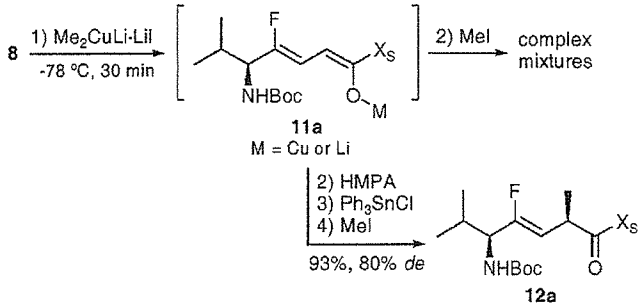

Scheme 2 Diastereoselective synthesis of a L-Val-L-Ala-type (*Z*)-fluoroalkene isostere.

Table 2 Diastereoselective synthesis of functionalized (*Z*)-fluoroalkene dipeptide isosteres by one-pot reduction/transmetalation/asymmetric alkylation

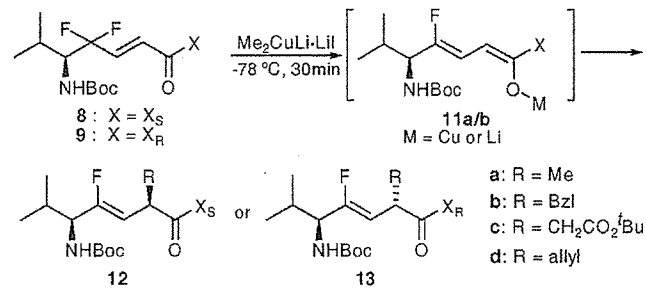

Entry	Electrophiles	Substrate	Products[a] (%)	de[b] (%)
1	MeI	**8**	**12a** (93)[c]	80
2	Bn–Br	**8**	**12b** (93)[c]	95
3	$BrCH_2CO_2{}^tBu$	**8**	**12c** (80)[c]	>95
4	Allyl–Br	**8**	**12d** (99)[c]	>95
5	$BrCH_2CH_2CO_2Me$	**8**	**10** (91)	—
6	MeI	**10**	**13a** (69)[c]	91
7	Bn–Br	**10**	**13b** (77)[c]	90
8	$BrCH_2CO_2{}^tBu$	**10**	**13c** (71)[c]	94
9	Allyl–Br	**10**	**13d** (79)[c]	92

[a] Isolated yield. [b] Determined by RP-HPLC of the purified products. [c] A trace amount of γ-alkylated products was detected by RP-HPLC.

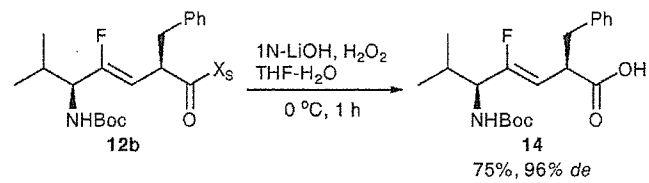

Scheme 3 Cleavage of the chiral auxiliary.

We thank Dr Terrence R. Burke Jr., NCI, NIH, USA for proofreading this manuscript. This research was supported in part by 21st Century COE Program 'Knowledge Information Infrastructure for Genome Science', a Grant-in-Aid for Scientific Research from the Ministry of Education, Culture, Sports, Science and Technology, Japan, the Japan Society for the Promotion of Science (JSPS) and the Japan Health Science Foundation.

Notes and references

‡ Fluoroalkene compounds obtained in this study have coupling constants in the range J_{HF} = 35.6–37.8 Hz. These values are consistent with those of compounds possessing (*Z*)-fluoroolefin units.[12]

§ The absolute configurations of the alkyl groups at the α-position were determined by circular dichroism measurements using an empirical rule after converting to the corresponding methyl esters.[13]

1 S. Oishi, T. Kamano, A. Niida, Y. Odagaki, N. Hamanaka, M. Yamamoto, K. Ajito, H. Tamamura, A. Otaka and N. Fujii, *J. Org. Chem.*, 2002, **67**, 6162; P. Wipf and J. Xiao, *Org. Lett.*, 2005, **7**, 103; J. Xiao, B. Weisblum and P. Wipf, *J. Am. Chem. Soc.*, 2005, **127**, 5742; H. Tamamura, K. Hiramatsu, S. Ueda, Z. Wang, S. Kusano, S. Terakubo, J. O. Trent, S. C. Peiper, N. Yamamoto, H. Nakashima, A. Otaka and N. Fujii, *J. Med. Chem.*, 2005, **48**, 380; C. L. Jenkins, M. M. Vasbinder, S. J. Miller and R. T. Raines, *Org. Lett.*, 2005, **7**, 2619.

2 R. J. Abraham, S. L. R. Ellison, P. Schonholzer and W. A. Thomas, *Tetrahedron*, 1986, **42**, 2101; T. Allmendinger, P. Furet and E. Hungerbühler, *Tetrahedron Lett.*, 1990, **31**, 7297; T. Allmendinger, E. Felder and E. Hungerbühler, *ACS Symp. Ser.*, 1991, **456**, 186; P. V. D. Veken, K. Senten, I. Kerèsz, I. D. Meester, A.-M. Lambeir, M.-B. Maes, S. Scharpè, A. Haemers and K. Augustyns, *J. Med. Chem.*, 2005, **48**, 1768; Y. Nakamura, M. Okada, A. Sato, H. Horikawa, M. Koura, A. Saito and T. Taguchi, *Tetrahedron*, 2005, **61**, 5741; A. Niida, K. Tomita, M. Mizumoto, H. Tanigaki, T. Terada, S. Oishi, A. Otaka, K. Inui and N. Fujii, *Org. Lett.*, 2006, **8**, 613.

3 A. Otaka, A. Yukimasa, J. Watanabe, Y. Sasaki, S. Oishi, H. Tamamura and N. Fujii, *Chem. Commun.*, 2003, 1834.

4 A. Otaka, E. Mitsuyama, H. Watanabe, H. Tamamura and N. Fujii, *Chem. Commun.*, 2000, 1081.

5 A. Otaka, H. Watanabe, E. Mitsuyama, A. Yukimasa, H. Tamamura and N. Fujii, *Tetrahedron Lett.*, 2001, **42**, 285; A. Otaka, H. Watanabe, A. Yukimasa, S. Oishi, H. Tamamura and N. Fujii, *Tetrahedron Lett.*, 2001, **42**, 5443.

6 A. Otaka, J. Watanabe, A. Yukimasa, Y. Sasaki, H. Watanabe, T. Kinoshita, S. Oishi, H. Tamamura and N. Fujii, *J. Org. Chem.*, 2004, **69**, 1634.

7 W. Oppolzer, D. Dupuis, G. Poli, T. M. Raynham and G. Bernardinelli, *Tetrahedron Lett.*, 1988, **29**, 5885.

8 T. Ibuka, T. Aoyagi, K. Kitada, F. Yoneda and Y. Yamamoto, *J. Organomet. Chem.*, 1985, **287**, C18; T. Ibuka, T. Aoyagi and Y. Yamamoto, *Chem. Pharm. Bull.*, 1986, **34**, 2417.

9 P. Girard, J. K. Namy and H. B. Kagan, *J. Am. Chem. Soc.*, 1980, **102**, 2693.

10 For some recent reviews, see: G. A. Molander, *Chem. Rev.*, 1992, **92**, 29; G. A. Molander, *Tetrahedron*, 1998, **54**, 3321; A. Krief and A.-M. Laval, *Chem. Rev.*, 1999, **99**, 745; P. Steel, *J. Chem. Soc., Perkin Trans. 1*, 2001, 2727.

11 P. A. Tardella, *Tetrahedron Lett.*, 1969, **10**, 1117; H. Nishiyama, K. Sakuta and K. Itoh, *Tetrahedron Lett.*, 1984, **25**, 223; H. Nishiyama, K. Sakuta and K. Itoh, *Tetrahedron Lett.*, 1984, **25**, 2487; M. Suzuki, A. Yanagisawa and R. Noyori, *J. Am. Chem. Soc.*, 1985, **107**, 3348; M. Suzuki, A. Yanagisawa and R. Noyori, *J. Am. Chem. Soc.*, 1988, **110**, 4718.

12 R. Waschüsch, J. Carran and P. Savignac, *Tetrahedron*, 1969, **52**, 14199.

13 T. Ibuka, H. Habashita, S. Funakoshi, N. Fujii, K. Baba, M. Kozawa, Y. Oguchi, T. Uehara and Y. Yamamoto, *Tetrahedron: Asymmetry*, 1990, **1**, 389.

European Journal of Neuroscience, Vol. 23, pp. 1120–1128, 2006 doi:10.1111/j.1460-9568.2006.04646.x

HIV-1 gp120 enhances giant depolarizing potentials via chemokine receptor CXCR4 in neonatal rat hippocampus

Alexander Kasyanov,[1,2] Hirokazu Tamamura,[3] Nobutaka Fujii[4] and Huangui Xiong[1,2]
[1]Neurophysiology Laboratory, Center for Neurovirology and Neurodegenerative Disorders, University of Nebraska Medical Center, Omaha, USA
[2]Department of Pharmacology and Experimental Neuroscience, University of Nebraska Medical Center, Omaha, NE 68198–5880, USA
[3]Department of Molecular Recognition, Institute of Biomaterials and Bioengineering, Tokyo Medical and Dental University, Tokyo, Japan
[4]Graduate School of Pharmaceutical Sciences, Kyoto University, Kyoto, Japan

Keywords: brain slices, EPSPs, HIV, patch clamp, Sprague–Dawley rat

Abstract

In the immature hippocampus, the giant depolarizing potentials (GDPs) are recurrent network-driven synaptic events generated by γ–aminobutyric acid (GABA), which in neonatal life is depolarizing and excitatory. The GDPs enable a high degree of synchrony in immature neurons and participate in activity-dependent growth and synapse formation. To understand how human immunodeficiency virus type one (HIV-1) infection in the immature brain impairs brain growth and development, we studied the effects of HIV-1 envelope glycoprotein, gp120, a viral toxin shed in abundance by infected cells, on spontaneous occurring GDPs recorded in the CA3 pyramidal cells in neonatal (P2–P6) Sprague–Dawley rat hippocampal slices using whole-cell patch technique. Bath application of gp120 produced a sustained enhancement of GDP frequency in a concentration-dependent manner without affecting passive membrane properties, suggesting that the site of action is most likely on neural network, other than on the recorded neurons. The gp120-induced enhancement of GDPs was blocked by T140, a highly specific antagonist for the chemokine receptor, CXCR4, indicating the involvement of CXCR4 in the gp120-induced increase of GDPs. Bath application of stromal cell-derived factor-1α (SDF-1α), the only CXCR4 ligand, mimicked the effects of gp120 on GDPs, supporting the engagement of CXCR4 receptors in the gp120-induced increase of GDP occurrence. Further studies revealed the involvement of protein kinase A/C in the gp120-induced enhancement of GDPs. These results demonstrate that gp120 enhances GDPs in the neonatal rat hippocampus. This enhancement may cause an excessive increase in intracellular calcium and resultant neuronal injury, leading to retardation of the brain and behavioural development as seen in paediatric AIDS patients.

Introduction

Infants and young children infected with human immunodeficiency virus type one (HIV-1) often have a higher incidence of HIV-1-associated encephalopathy (HE), a devastating complication of HIV-1 infection in the central nervous system (CNS; Ammann, 1994; Belman, 1994). HE is manifested as a well-defined triad of clinical features, i.e. impaired brain growth, loss of developmental milestones with cognitive deterioration, and symmetrical motor deficit (Epstein *et al.*, 1986; Belman *et al.*, 1988; Mintz & Epstein, 1992). A recent large cohort study revealed that approximately 10% of children developed HE during the first year of HIV-1 infection (in contrast to 0.3% in adults) and cumulative incidence at seven years postinfection reached 16% in children and 5% in adults (Tardieu *et al.*, 2000). The frequent occurrence of HE in these young patients adds significantly to the morbidity of the disease (Belman *et al.*, 1993). Nevertheless, the mechanisms underlying clinical onset of HE in children remain unknown. It is commonly believed that the pathogenesis of HE in paediatric patients is similar to the pathophysiologic mechanisms of HIV-1-associated dementia (HAD) in adult patients, involving viral infection, immune activation of brain mononuclear phagocytes (MPs, brain macrophages and microglia), and resultant release of diffusible viral and cellular toxins, leading to neuronal and astrocytic dysfunction and/or death (Gendelman *et al.*, 1997; Nath, 2002). Amongst these toxins is the HIV-1 envelope glycoprotein, gp120, one of the major viral toxins released from HIV-1-infected MPs. Accumulating evidence suggests that gp120 plays an important role in HIV-1-associated neuropathology in HAD and HE.

HIV-1 gp120 induces neurotoxic activity in cultures of rodent hippocampal and human embryonic neurons (Dawson *et al.*, 1993; Lannuzel *et al.*, 1995; Meucci & Miller, 1996), as well as in rodent brains *in vivo* (Bagetta *et al.*, 1996b; Bansal *et al.*, 2000). Systemic administration of gp120 in neonatal rats or intracerebroventricular injection in adult rats resulted in deleterious effects on the brain (Hill *et al.*, 1993; Bagetta *et al.*, 1996a; Acquas *et al.*, 2004). Overexpression of gp120 in the brains of transgenic mice produced widespread neuronal dendritic vascularization and loss of neuronal populations (Toggas *et al.*, 1994). Thus, gp120 has been proposed to

Correspondence: Dr Huangui Xiong, [2]Department of Pharmacology and Experimental Neuroscience, as above.
E-mail: hxiong@unmc.edu

Received 24 August 2005, revised 21 December 2005, accepted 23 December 2005